Spring 2020

Diatom Community Composition Shifts Driven by Coherent Cyclonic Mesoscale Eddies in the California Current System

Zuzanna Maria Abdala
Old Dominion University, zuzyabdala@gmail.com

DIATOM COMMUNITY COMPOSITION SHIFTS DRIVEN BY COHERENT

CYCLONIC MESOSCALE EDDIES IN THE CALIFORNIA CURRENT SYSTEM

by

Zuzanna Maria Abdala
B.A. May 2014, George Mason University

A Thesis Submitted to the Faculty of
Old Dominion University in Partial Fulfillment of the
Requirements for the Degree of

MASTER OF SCIENCE

OCEAN AND EARTH SCIENCES

OLD DOMINION UNIVERSITY
May 2020

Approved by:

P. Dreux Chappell (Director)

Fred C. Dobbs (Member)

Sophie Clayton (Member)

ABSTRACT

DIATOM COMMUNITY COMPOSITION SHIFTS DRIVEN BY COHERENT CYCLONIC

MESOSCALE EDDIES IN THE CALIFORNIA CURRENT SYSTEM

Zuzanna Maria Abdala
Old Dominion University, 2020
Director: Dr. P. Dreux Chappell

The California Current System (CCS) is characterized by an equatorward flowing eastern boundary current, as well as seasonal wind-driven coastal upwelling which supplies nutrient-rich waters to the surface and drives high coastal productivity. Cyclonic mesoscale eddies form off the coast in the CCS where they trap the highly productive upwelled coastal waters, along with their resident planktonic communities, and transport them offshore into the more oligotrophic California Current waters. The interaction between waters within and outside of the eddies is limited, and so the eddies act as natural mesocosms, where the resident phytoplankton population undergo ecological succession as the eddy ages. Diatoms, a unicellular and eukaryotic subgroup of phytoplankton, have high sensitivities to changes in their environment, particularly temperature and nutrient distributions. In this study, I examine how diatom communities trapped within mesoscale eddies in the CCS evolve in response to environmental shifts as they travel offshore.

In a transect that bisected two cyclonic eddies off the coast of northern California near Cape Mendocino, diatom samples were collected and later sequenced using high throughput sequencing. Although the eddies both originated in broadly the same location, they had formed 2 and 10 months previous to sampling, respectively. Because of this difference in the age of the eddies, I can approximate the time evolution of a single CCS eddy by comparing their biogeochemical and ecological characteristics. The older, offshore eddy was low in

macronutrients, nitrate-limited, low in Fe, and lower in diversity, the last result largely driven by the relative abundance of a single *Rhizosolenia* species. *Rhizosolenia* accounted for over 50% of the diatom community in 5 out of 8 offshore eddy stations, with one of these stations characterized by nearly 75% *Rhizosolenia*. Our results suggest that the *Rhizosolenia* species present in the offshore eddy is one that bypasses nitrate limitation by forming vertically migrating mats. I also found elevated relative abundances of *Pseudo-nitzschia cf. sp.* and *Thalassiothrix sp.* in the offshore eddy. The younger, nearshore eddy was higher in macronutrients, Fe-limited, and higher in diversity. Top abundances for this eddy include *Pseudo-nitzschia sp.*, *Fragilariopsis kerguelensis*, *F. cf. kerguelensis*, *Thalassiosira ritscheri*, *Asteromphalus sp.*, and *T. oestrupii*. Our results show that the biogeochemistry and diatom community structure within cyclonic eddies evolve as the eddies move offshore from the coast. The high-nutrient coastal waters are initially dominated by coastal diatoms known to have higher nutrient requirements. As the nutrients within the eddy are drawn down over time, species equipped with low-nutrient adaptations can become dominant. The combined effect of transport by, and ecological succession within the eddies is likely a key factor in mediating carbon cycling and export across the wider CCS region.

This thesis is dedicated to my family and friends.

ACKNOWLEDGMENTS

I would like to sincerely thank and honor my committee members, Drs. Chappell, Clayton, and Dobbs. Without their vast knowledge, keen insight, and invaluable words of wisdom, I don't think I would have made it out alive. I am forever grateful for your existence and hope to one day grow up to be just like you.

I would also like to give special thanks to my advisor in both academics and life in general, Dr. Chappell. She provided me with so many tools and opportunities to help me shine, even through major hurdles. I am forever grateful to be her first grad student and hope that I made her proud and continue to do so. Many thanks for showing me how awesome diatoms are, for encouraging me to step out of my comfort zone, for whisking me off to the Southern Ocean, for giving me emergency chocolate while crying IN the Southern Ocean, and for believing in me. You're the best.

To my lab crew, I owe a million thanks. To my friend and lab manager Kim Powell, for teaching me all the greatest lab procedures, having enough patience to answer my endless questioning, and for being a fantastic person I will always look up to. And to my labmate Sveinn Einarsson, for showing me the slickest programming shortcuts, being a source of sanity in the chaos of grad school and being a wonderful friend.

TABLE OF CONTENTS

LIST OF FIGURES

INTRODUCTION

Phytoplankton are a group of photoautotrophic microorganisms that are geographically cosmopolitan, occupying most aquatic habitats around the world (Vanormelingen, Verleyen, & Vyverman, 2007). Marine phytoplankton account for only 1-2% of the total plant biomass globally yet contribute ~ 40% of earth's total fixed carbon (Falkowski, 1994). Diatoms are a subgroup of phytoplankton that are unicellular and eukaryotic. They contribute ~ 25% of the global primary production (Sumper & Brunner, 2006), and ~ 40% of the primary production in the oceans (Falkowski, Barber, & Smetacek, 1998). Out of all the eukaryotic marine phytoplankton globally, diatoms are known to be the greatest in abundance and highest in diversity (Bowler, Vardi, & Allen, 2010; Kooistra, Gersonde, Medlin, & Mann, 2007; Lewitus, Bittner, Malviya, Bowler, & Morlon, 2018). Previously, 200,000 diatom species were estimated to exist worldwide (Mann & Droop, 1996), though a recent estimate suggests a more conservative range of 30,000 to 100,000 diatom species (Mann & Vanormelingen, 2013). Diatom productivity has a significant control on fixed carbon availability for other trophic levels (Ducklow, Steinberg, & Buesseler, 2001; Falkowski et al., 1998), making diatoms key players in the success of fisheries (Chenillat, Franks, & Combes, 2016).

The role of diatoms in the biological pump is important because of the transfer of carbon to other trophic levels (carbon cycling) and the removal of carbon from the surface waters to the ocean floor through sinking diatom frustules, fecal pellets from primary consumers, or aggregates (carbon export) (Brown et al., 2008). This carbon transfer results in a strong carbon gradient at the atmosphere-ocean surface interface, allowing carbon in the form of CO_2 to be removed from the atmosphere (Falkowski et al., 1998). In a studying examining a collection of 17 marine diatom species, the rate of uptake of carbon (predominantly through bicarbonate)

varied significantly among species (Martin & Tortell, 2008). Therefore, the rate of carbon cycling and export from surface oceans is significantly influenced by the community composition of diatoms (Brown et al., 2008).

Examining diatom community composition can also provide insight into prevailing environmental conditions. Nutrient distributions can fluctuate rapidly for a variety of reasons, including drawdown from primary producers, ocean circulation, and dust deposition (Ducklow et al., 2001; Falkowski, 1995). Nutrient delivery—or lack thereof—determines the amount of biomass an environment can support. Regions with higher frequencies of nutrient delivery, such as eastern boundary upwelling systems (EBUS), can support both larger abundances of biomass (blooms) and larger cells (Hood, Abbott, Huyer, & Kosro, 1990). Regions with lower frequencies of nutrient delivery, such as open oceans, are commonly in a nutrient-limited state and generally have lower biomass and cell sizes (Bibby, Gorbunov, Wyman, & Falkowski, 2008; Brown et al., 2008). Diatoms have high sensitivities to changes in their surroundings, including circulation, temperature, light availability and nutrient distributions (Heil, Revilla, Glibert, & Murasko, 2007)—so much so that they are commonly used as a bioindicator for environmental health in freshwater ecosystems like lakes, rivers, and streams (Visco et al., 2015). Over time, some diatoms have developed adaptations to help them survive—and even thrive—under nutrient limitation (Bowler et al., 2010). The presence, absence, or dominance of the known diatoms with specific adaptations can supplement nutrient concentration measurements to reveal a clearer picture of the environmental conditions.

Cell counts and light microscopy lack in both specificity and accuracy in species-level identifications (Kaczmarska, Lovejoy, Potvin, & Macgillivary, 2009; Tomas, 1997; Zimmermann, Glockner, Jahn, Enke, & Gemeinholzer, 2015). In a study that compared diatom

identification through high-throughput sequencing and light microscopy, the sequencing technique was able to recover 270 identified taxa, while the light microscopy only recovered 103 taxa (Zimmermann et al., 2015). *Skeletonema costatum* sensu lato (s. l.) (Greville) Cleve, previously described as morphologically and physiologically versatile, has since been parsed into at least nine distinct species using sequencing (Kooistra et al., 2008). The genus *Attheya* is commonly misidentified as the genus *Chaetoceros*, which it is morphologically similar to (Crawford, Hinz, & Koschinski, 2000), though this issue is mostly eliminated with sequencing techniques (Hardge et al., 2017). For these reasons, a high-throughput sequencing technique (Chappell et al., 2019) was utilized in this experiment to examine diatom community composition.

The California Current System (CCS) is characterized by a collection of currents, upwelling, downwelling, and mesoscale activity that is typical of EBUS regions. The prevailing current is the California Current (CC), which has a width of 1000 km, depth of 300 m, and flows equatorward at a speed of 10-30 cm/s (Combes et al., 2013; Kurian, Colas, Capet, McWilliams, & Chelton, 2011), bringing colder, fresher water southward along the western coast of the continent. The California Undercurrent (CUC), which is only 10-40 km in width (Combes et al., 2013), flows adjacent to the CC along the continental slope in a poleward direction 100-400 m below the surface (Combes et al., 2013; Kurian et al., 2011), distributing warmer, nutrient-rich waters northward. During the winter and fall, a weaker, nearshore, and poleward current reappears, known as the Davidson Current (Kurian et al., 2011), displacing coastal communities north of their origins.

Vertical transport of nutrients into the euphotic zone occurs from two main sources—the primary source being shoaling of isopycnals (Biller & Bruland, 2014) and the secondary source

is coastal upwelling (Owen, 1980). The seasonal shifts of wind direction in this region controls the presence and absence of upwelling, which impacts nutrient distributions at the surface. In the summer, the winds blow towards the equator (Du & Peterson, 2013), which leads to Ekman transport offshore. The displacement of water offshore causes deep water to take its place at the surface, resulting in coastal upwelling. In the winter, the prevailing winds switch to a poleward direction (Du & Peterson, 2013), causing Ekman transport onshore and downwelling along the coast. Freshly upwelled waters have nitrate, silicate, and phosphate concentrations that range from 15-35 μM, 15-45 μM, and 1.3-2.6 μM respectively (Bruland, Rue, & Smith, 2001). Because of the coastal upwelling dynamics providing nutrient delivery to the surface with high frequency, the CCS is one of the most biologically productive regions in the world (Capone & Hutchins, 2013; Lachkar & Gruber, 2012) and provides a disproportionate amount of primary production compared to surrounding regions (Chenillat et al., 2016). Upwelled waters can lead to chlorophyll *a* values between 10-35 μg/L (Bruland et al., 2001). In many areas of the CCS, the silicate concentration far exceeds the nitrate concentration, allowing for a phytoplankton community that is diatom-dominant (Chavez et al., 1991; Du & Peterson, 2013; Hood et al., 1990; Venrick, 2009; Wilson et al., 2008). Nutrient-rich coastal waters in the CCS are home to elevated proportions of larger (Bibby et al., 2008; Bruland et al., 2001; Hood et al., 1990), centric (Aizawa, Tanimoto, & Jordan, 2005) diatoms compared to open ocean ecosystems. The convergence of several CCS nearshore dynamics, including coastal upwelling, mixing from opposing currents, and river outflows, has an impact on the phytoplankton and diatom community compositions (Du & Peterson, 2013). The CCS also has strong seasonality, which can dramatically alter the structure of the diatom communities depending on the presence, absence, or strength of upwelling (Du & Peterson, 2013).

In addition to upwelling and downwelling, the CCS is high in both strength and frequency of mesoscale activity (Chenillat et al., 2016), which plays a significant role in the movement of water in the region. Eddy formation occurs from baroclinic instability (Bibby et al., 2008; Kurian et al., 2011), which can result from many different factors, including coastline irregularities, upwelling filaments, seafloor topography, wind forcings, the shearing from opposing currents, or a combination of these (Batteen, Cipriano, & Monroe, 2003). One area along the California coast where eddies commonly form is Cape Mendocino, an area with a mountainous headland and complex bathymetry attributed to a triple junction (Hoover & Tréhu, 2017), elevated eddy kinetic energy (Batteen et al., 2003), high frequency of filaments (Marchesiello, McWilliams, & Shchepetkin, 2003; Nagai et al., 2015), and is the westernmost point of the California coast (Smith, 1999). Cyclonic eddies in the CCS are most commonly formed in the fall (Chenillat et al., 2018; Chenillat et al., 2016), which could be a result of the fall reappearance of the weaker, poleward Davidson Current or the fall strengthening of the CUC (Kurian et al., 2011). Recent models have shown eddies in the CCS contain water from both northern (via the CC) and southern (CUC) origin (Chenillat et al., 2018; Combes et al., 2013). CCS eddies are highly nonlinear compared to eddies globally (Kurian et al., 2011), meaning the rotational speed is much faster than the speed of offshore propagation, severely limiting exchange with surrounding waters (Chenillat et al., 2018). Upwelled nutrients are advected offshore via filaments—responsible for most of the nutrient transport within the first 100 km from shore—and surface and subsurface eddies—responsible for transport 200 to 800 km offshore (Combes et al., 2013; Nagai et al., 2015). In fact, 50% of the total transport of nitrate in the CCS can be attributed to eddies (Chenillat et al., 2018; Chenillat et al., 2016). Coastal diatoms, which also become entrained into eddies, are known to have higher macro- and

micronutrient requirements for growth (Marchetti, Maldonado, Lane, & Harrison, 2006), making them more susceptible to nutrient depletion (Hood et al., 1990). Because eddies are effective in transporting coastal water offshore (Combes et al., 2013), they can advect the nutrient-rich waters from coastal upwelling to benefit a larger area, hundreds of kilometers offshore (Bruland et al., 2001). This mosaic of mesoscale (and sub-mesoscale) processes creates many sharp salinity and nutrient fronts (Nagai et al., 2015). Additionally, because of the strong seasonality of the winds, currents, and upwelling, nutrient distributions are also strongly seasonal (Du & Peterson, 2013).

Mesoscale eddies are high frequency structures in the CCS and are known to have a direct control on coastal ecosystems (Chenillat et al., 2016; Chenillat et al., 2015). CCS eddies are also highly efficient in trapping parcels of coastal water and transporting them offshore (Chenillat et al., 2016; Combes et al., 2013). These eddy parcels contain upwelled waters high in nutrients (Kurian et al., 2011), and diatom communities high in diversity (Goebel, Edwards, Zehr, Follows, & Morgan, 2013; Venrick, 2009). CCS cyclonic eddies increase productivity to coastal-like levels (Benitez-Nelson et al., 2007; Brown et al., 2008), increase the phytoplankton photosynthetic efficiency (Bibby et al., 2008), sustain higher productivity for extended periods up to one year and up to 800 km offshore (Chenillat et al., 2016), and have a substantial role in controlling the carbon cycling and export in the CCS (Benitez-Nelson et al., 2007; Brown et al., 2008). These pockets of elevated productivity can be the primary source of nourishment for coastal fisheries (Brown et al., 2008), controlling their success or collapse (Chenillat et al., 2016).

Because of the entrapment of coastal waters, combined with longer lifespans of cyclonic eddies (Kurian et al., 2011), the coastal diatom communities within cyclones can undergo an

ecological succession as the eddy ages and travels offshore (Brown et al., 2008; Owen, 1980). In a spatial study, diatom communities of similar composition were found along concentric rings, with each ring in a different stage of succession (Owen, 1980). In a temporal study, larger-celled, coastal diatoms were succeeded by smaller-celled, open ocean diatoms in a Hawaiian lee cyclonic eddy ecosystem, attributed to the depletion of nutrients and an environmental shift more suited to smaller cells (Brown et al., 2008). In addition to smaller diatoms, long-lived eddies may also be suitable for diatom species with physiological adaptations to nutrient limitation, such as vertical migrators or those with dinitrogen-fixing endosymbionts (Wilson & Qiu, 2008). Because of the wide spatial and temporal variability in community structures within eddies, there is a need to better understand the processes that drive community shifts (Brown et al., 2008).

The combination of high frequency mesoscale activity, strong seasonality, and an extensive presence of diatoms makes the CCS an ideal region to examine how diatom communities respond to nutrient pulses and ocean dynamics. The current study aims to gain a better understanding of how eddy dynamics in the CCS impact diatom communities. It examines a suite of ecological factors occurring in two cyclonic (rotating counterclockwise) CCS eddies— an inshore eddy that was two months old and an offshore eddy that was ten months old, both of which formed near Cape Mendocino. Because CCS eddies are highly non-linear, they are efficient in trapping coastal waters with high nutrients and diverse diatom communities and encouraging ecological succession. In sampling two eddies that differ in age yet originate from the same region, comparing the biological contents of these eddies can serve as a proxy for a long-term, *in situ* study of ecological succession of diatoms within a CCS eddy.

METHODS

SAMPLE COLLECTION

Samples from transects were collected off the coast of northern California, just south of Cape Mendocino, 13-14 July 2014 on the R/V Melville cruise (MV 1405). The cruise track (Figure 1) began 430 km from the coastline of Northern California, traveled northeast, and pivoted midway to allow for sampling through the centers of two cyclonic eddies. For simplicity, the two eddies (Figure 1) will be identified as eddy I, the younger eddy, and eddy II, the older eddy. A trace metal clean surface tow-fish system (Bruland, Rue, Smith, & DiTullio, 2005) was used to collect water from 3-5 m depth while the ship was underway (~10 knots). Samples for DNA analysis were collected at roughly 1-hour intervals. One to two liters of water were filtered onto 25 mm diameter, 3 μm polyester filters using a Masterflex peristaltic pump. Filters were placed in 2 mL screw-cap tubes with 400 μL of Qiagen® RLT Plus Buffer (Qiagen, Germany), frozen in liquid N_2, and stored at –80 °C until DNA extraction.

ENVIRONMENTAL DATA

Surface temperature and salinity were measured using the R/V Melville's SBE 21 Thermosalinograph system (SeaBird Electronics). Water samples for both surface macronutrient analyses and surface dissolved Fe (dFe) analyses were collected from the tow-fish system (Bruland et al., 2005) and filtered through an acid-cleaned, seawater-flushed 0.2 μm Acropak filter capsule (Pall 500, Fisher Scientific). Nitrate + nitrite, phosphate, and silicate were analyzed onboard using a Lachat QuickChem 800 Flow Injection Analysis System following standard spectrophotometric methods (Parsons, 1984). Surface dFe was analyzed onboard using a chelating method, described in detail by Till et al. (2019).

DNA EXTRACTION

Filters were extracted using the Qiagen® Allprep RNA/DNA co-extraction with an additional bead-beating step and homogenization using the QIAshredder column (Qiagen, Germany). Extracted DNA was diluted at least 1:10 or to 3 ng/µL. The V4 region of the 18S rDNA was amplified in triplicate using primers designed to target diatoms (Zimmermann, Jahn, & Gemeinholzer, 2011) that were modified to include the Illumina overhang adapter sequences for two step amplicon sequencing (http://www.illumina.com/content/dam/illumina-support/documents/documentation/chemistry_documentation/16s/16s-metagenomic-library-prep-guide-15044223-b.pdf). 25 µL PCR reactions consisted of 2.5 µL of diluted DNA, 1.25 µL of each 5 µM primer, 7.5 µL of PCR-grade water, and 12.5 µL Phusion GC MasterMix (Life Technologies Corporation, Carlsbad, CA, USA). PCR reactions were performed using a SimpliAmp Thermal Cycler (Life Technologies Corporation, Carlsbad, CA, USA). PCR conditions consisted of 98°C for 3 minutes, then 35 cycles of [98°C for 15 seconds, 62°C for 15 seconds, 72°C for 30 seconds], then a final 72°C for 5 minutes. Successfully amplified triplicate samples were pooled and purified using Agencourt AMPure XP beads (Beckman Coulter, Brea, CA, USA). An agarose gel was then used to verify presence and size of the amplicon. A secondary PCR (3 minutes at 72 °C, 30 seconds at 98 °C, 6 cycles of [10 seconds at 98 °C, 30 seconds at 63 °C], and finally 3 minutes at 72 °C) was conducted using Nextera indexed adapters. PCR product was purified again with AMPure XP beads, agarose gel verified, and diluted to 3.2 ng/µL concentration in preparation for a pooling of a multiplexed library to be sequenced. Nextera tagged samples were pooled and paired-end sequenced at the Illumina MiSeq sequencer at Old Dominion University using the 2x300 bp sequencing kit.

SEQUENCE PROCESSING

Sequences were de-multiplexed and imported into the CLC Genomics Workbench (Qiagen, Germany). Reads were imported in pairs, trimmed, and merged in CLC before being exported in fasta format. Parameters for trimming were as follows: no ambiguous nucleotides allowed, quality limit 0.02, and discard reads < 150 nucleotides in length post trimming. Read merging parameters were as follows: mismatch cost = 1, minimum score = 8, gap cost = 2, and maximum unaligned end matches = 5. Following the merge, reads were searched for the primer sequences and any merged reads without the primers were discarded. The remaining merged reads had the primers trimmed off. A final trimming step had the following parameters: no ambiguous nucleotides, quality limit = 0.05; reads were discarded if they were not within the range of 390-415 nucleotides in length. Reads were exported out of CLC as single fasta files. Mothur, an open source software package optimized for bioinformatics usage (Schloss et al., 2009a), was selected to streamline and organize sequence data formatting for optimal node representative identification using shell scripting. Reads were screened using the classify.seqs tool of mothur (Schloss et al., 2009b) using an in-house database that combined stramenopile 18S sequences from NCBI (downloaded as of May 10, 2016) and the SILVA eukaryote 18S database. The get.lineage mothur tool was used to select all reads that were classified as Bacillariophyta. Due to the variation in reads per sample, a normalization randomized subset of 22,000 reads per sample was extracted. The output from mothur was then used in the minimum entropy decomposition (MED) pipeline (Eren et al., 2015). This clustering algorithm partitioned the randomized subset of sequences for each sample into operational taxonomic units (OTUs) that MED refers to as nodes. The representative sequence for each OTU was used as the input in a nucleotide BLAST (Altschul, Gish, Miller, Myers, & Lipman, 1990) against an in-house database that combined stramenopile 18S sequences from NCBI (updated as of

June 26, 2017) and the SILVA eukaryote 18S database sequences. Due to trimming parameters, some sequences that were otherwise identical (indicating they were from the same species) were a base or two shorter in length and ended up being pooled into different OTUs. To deal with this issue, OTUs were pooled (i.e., read counts combined) if they had <1 % percent identity difference. OTUs were classified to the species level if they had > 99% percent identity to a classified organism. Because of the sequence similarity of the 18S rDNA, any OTU sequences with percent identity between 97-99% were classified as "*Genus* cf. *species*" to signify that the OTU was similar to a known species. OTU sequences with percent identity < 97% were only classified to the genus level. OTU sequences identified to the genus level under the same genus were given the designation "-sp." followed by a number to indicate a difference in species.

COMMUNITY COMPOSITION ANALYSES

OTU counts were imported into PRIMER 7 (PRIMER-E Ltd, Plymouth, UK), log(X+1) transformed, and a matrix of Bray-Curtis similarity coefficients (Bray & Curtis, 1957) was utilized to compare the relative abundance data for each station. A dendrogram was generated from the Bray-Curtis similarity matrix using the group average clustering mode. The ecological indices used to assess community diversity were the Shannon-Wiener diversity index (Shannon, 1948) and richness. Diversity and richness calculations were based on the OTU counts at each station. Composition columns were created for each station in Prism (GraphPad Prism version 7 for Macintosh).

STATISTICAL ANALYSES

Statistical tests were performed for a set of select variables (Appendix Table 1), including temperature, salinity, fluorescence, nitrate, silicate, phosphate, silicate:nitrate, dFe:nitrate, diversity, relative abundance of *Rhizosolenia sp. 1*, and wind speed. Variables were first tested for normality using skewness, kurtosis (Pearson, 1905; Westfall, 2014), and Kolmogorov–Smirnov (Appendix Table 1A) (Lilliefors, 1967; Massey, 1951). Statistical tests were conducted comparing the variables among three groups, eddy I, eddy II, and non-eddy. For variables with a normal distribution, a one-way analysis of variance (ANOVA) was performed (Appendix Table 1B) (Fisher, 1921). For variables with a non-normal distribution, a Kruskal-Wallis test was performed (Appendix Table 1C) (Kruskal & Wallis, 1952). Post hoc tests were performed to obtain detailed differences between each set of groups – eddy I vs. eddy II, eddy I vs. non-eddy, and eddy II vs. non-eddy (Appendix Table 2). Tukey's honestly significant difference (HSD) post hoc test was performed after all ANOVA tests (Tukey, 1976). Dunn's post hoc test was performed after all Kruskal-Wallis tests (Dunn, 1964).

RESULTS

ENVIRONMENTAL DATA

The geographical locations of the stations are shown superimposed on gridded sea level anomaly (SLA; grey contours) from the Aviso dataset for satellite altimetry data for July 10, 2014 (Figure 1; http://www.aviso.altimetry.fr/). A monthly composite of chlorophyll *a* for July 2014 from the MODIS instrument (moderate resolution imaging spectroradiometer) aboard the Terra and Aqua satellites is also shown (colors; Figure 1); values ranged from 0.1 mg m^{-3} to 10 mg m^{-3}. Contours show SLA differences of 25 cm, with dashed lines representing negative SLAs and solid lines representing positive SLAs in comparison to the mean sea level height. SLA ranged from + 2.5 m to – 1 m, with concentric negative SLAs (dashed contours) showing cyclonic eddies. The highest values for chlorophyll were found along the coast. The transect passed through the centers of two cyclonic eddies. From this point on, stations 15-22 (nearshore) will be referred to as "eddy I" and stations 2-9 (offshore) will be referred to as "eddy II." Through searching for coherency in the eddy formation retroactively in week-by-week images from the Aviso dataset, eddy I was confirmed to have separated from the coast approximately 2 months prior to sampling and eddy II separated from the coast approximately 10 months prior to sampling.

The surface temperature (Figure 2A) across the transect ranged from 12.7°C to 17.2°C, with warmer water offshore and cooler water nearshore. The average temperature of eddy I was 13.8°C ± 0.6°C, eddy II averaged 16.1°C ± 0.4°C, and in between eddies, the average temperature was 15.8°C ± 0.9°C. Temperature was significantly different (Appendix Table 1B) across the three regions (eddy I, eddy II, and non-eddy), $F(2, 18) = 45.1$; *p*-value < 0.05.

Figure 1. Geographical location of the study site. Grey contours represent sea level anomaly. Stations are numbered in succession, beginning with Station 1 at the most-western point to Station 22 at the most-eastern point. Logscale chlorophyll concentration is shown in color.

Post hoc tests reveal that the differences in temperature between eddies I and II and between eddy I and non-eddy were significant (p-values < 0.01; Appendix Table 2) while the difference between eddy II and non-eddy was not significant. The surface salinity (Figure 2B) across the transect ranged from 32.36 to 33.12, with similar average salinities for eddies I and II (33.00 ± 0.05

and 32.80 ± 0.09, respectively). In between eddies, the salinity was lower, with an average of 32.44

± 0.13. Salinity was significantly different (Appendix Table 1B) across the three regions (eddy I,

eddy II, and non-eddy), $F(2, 18) = 40.1$; p-value < 0.05. Post hoc tests reveal that the differences in

salinity between each region pairing were significant (p-values < 0.05; Appendix Table 2). The

surface fluorescence (Figure 2C) ranged from $0.17 \ \mu g \ L^{-1}$ to $3.06 \ \mu g \ L^{-1}$. Averages showed elevated

fluorescence in eddies I and II ($1.71 \ \mu g \ L^{-1} \pm 0.66 \ \mu g \ L^{-1}$ and $1.50 \ \mu g \ L^{-1} \pm 0.37 \ \mu g \ L^{-1}$, respectively)

compared to non-eddy stations ($0.32 \ \mu g \ L^{-1} \pm 0.17 \ \mu g \ L^{-1}$). Fluorescence was significantly different

(Appendix Table 1B) across the three regions (eddy I, eddy II, and non-eddy), $F(2, 18) = 8.1$; p-

value < 0.05. Post hoc tests reveal that the difference in fluorescence between eddies I and II was

not significant while the differences between eddy I and non-eddy and between eddy II and non-

eddy were significant (p-values <0.01; Appendix Table 2). Density values (Figure 3) were

calculated in ODV using conservative temperature and absolute salinity. Density was significantly

different (Appendix Table 1B) across the three regions (eddy I, eddy II and non-eddy), $F(2, 18) =$

85.3; p-value < 0.05. Post hoc tests reveal that the differences in density between each region pairing

was significant (p-values < 0.05; Appendix Table 2).
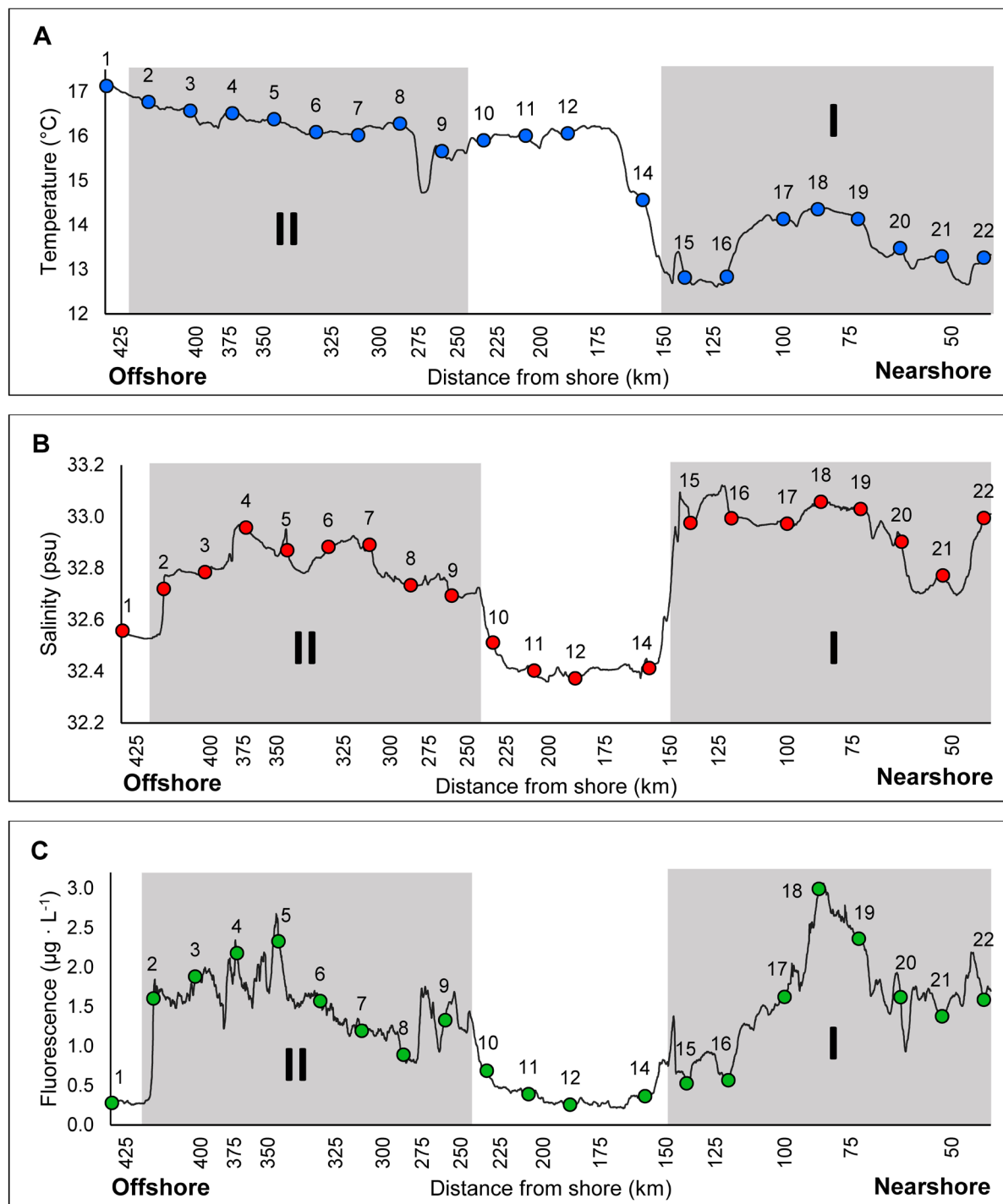
Figure 2. Underway measurements of (**A**) sea surface temperatures (°C), (**B**) surface salinity (psu), and (**C**) surface fluorescence (μg · L⁻¹). Grey boxes demarcate the boundaries of eddies I and II. The numbers above the datapoints represent the station number.
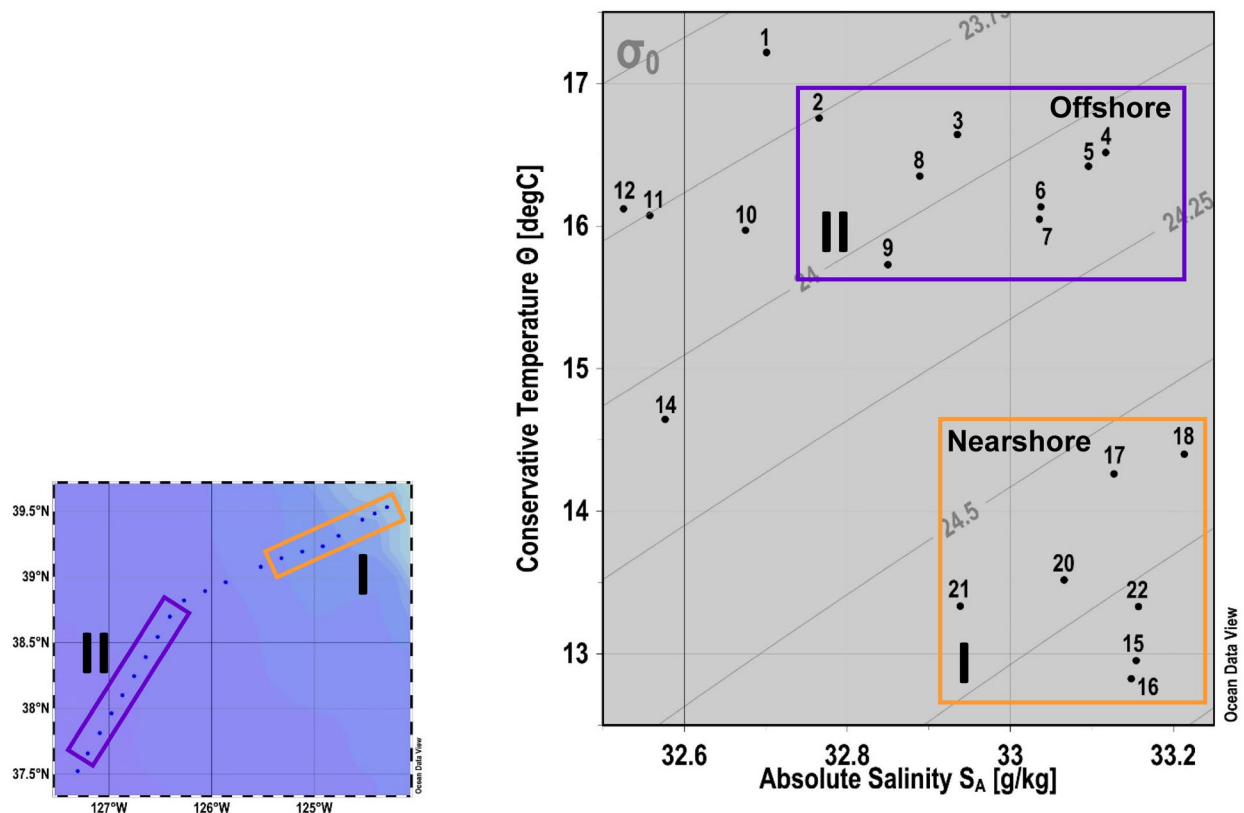
Figure 3. Density values calculated from absolute salinity and conservative temperature. Boxes have been added around stations within eddies I and II.

Nutrients

Nitrate concentrations (Figure 4A) ranged from 0.05 μmol kg^{-1} at station 11 to 8.28 μmol kg^{-1} at station 16 and were, on average, more than 6 times higher in eddy I (average of 5.24 μmol kg^{-1} ± 1.95 μmol kg^{-1}), while eddy II showed near-depleted levels of nitrate (average of 0.82 μmol kg^{-1} ± 0.83 μmol kg^{-1}). Nitrate concentrations were significantly different (Appendix Table 1B) across the three regions (eddy I, eddy II, and non-eddy), $F(2, 18) = 38.3$; p-value < 0.05. Post 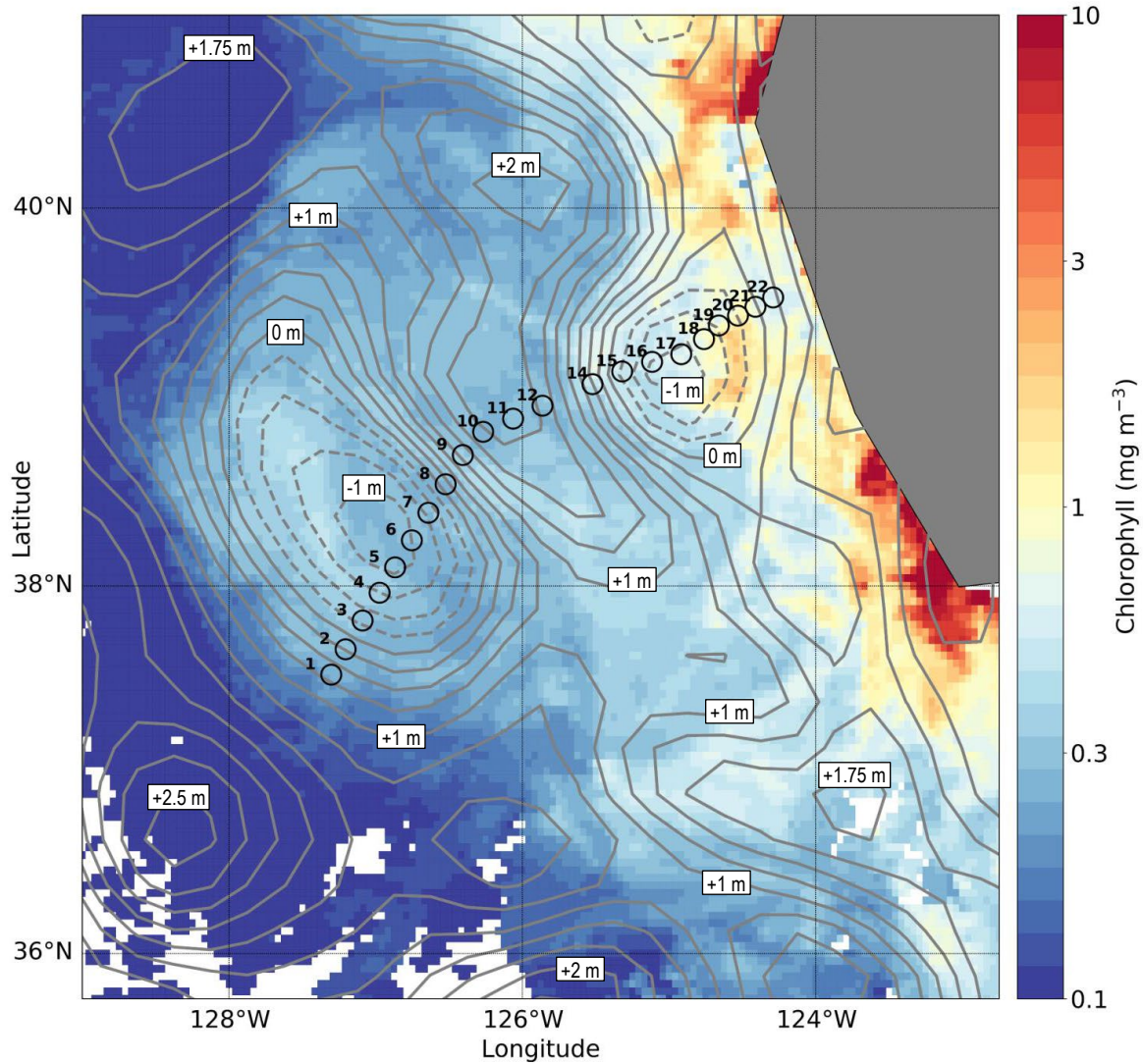hoc tests reveal that the differences in nitrate concentrations between eddies I and II and between eddy I and non-eddy were significant (p-values < 0.01; Appendix Table 2) while the difference between eddy II and non-eddy was not significant. Silicate measurements (Figure 4B) ranged from 0.94 μmol kg^{-1} (at station 5) to 4.09 μmol kg^{-1} at station 22. Average silicate in eddy I, 3.28 μmol kg^{-1} ±

0.67 µmol kg^{-1}, was more than double the average seen in eddy II, 1.73 µmol kg^{-1} ± 0.50 µmol kg^{-1}. Silicate concentrations were significantly different (Appendix Table 1B) across the three regions (eddy I, eddy II, and non-eddy), $F(2, 18) = 17.1$; p-value < 0.05. Post hoc tests reveal that the differences in silicate concentrations between eddies I and II and between eddy I and non-eddy were significant (p-values < 0.01; Appendix Table 2) while the difference between eddy II and non-eddy was not significant. Phosphate measurements (Figure 4C) ranged from 0.29 µmol kg^{-1}, observed at stations 8, 11, and 12, to 0.80 µmol kg^{-1} at station 16. The average for phosphate in eddy I, 0.63 µmol kg^{-1} ± 0.11 µmol kg^{-1}, was nearly double that of eddy II, 0.33 µmol kg^{-1} ± 0.03 µmol kg^{-1}. Phosphate was significantly different (Appendix Table 1B) across the three regions (eddy I, eddy II, and non-eddy), $F(2, 18) = 47.1$; p-value < 0.05. Post hoc tests reveal that the differences in phosphate concentrations between eddies I and II and between eddy I and non-eddy were significant (p-values < 0.01; Appendix Table 2) while the difference between eddy II and non-eddy was not significant. I observed a sharp increase in all macronutrient concentrations at the nearshore eddy front, between stations 14 and 15.
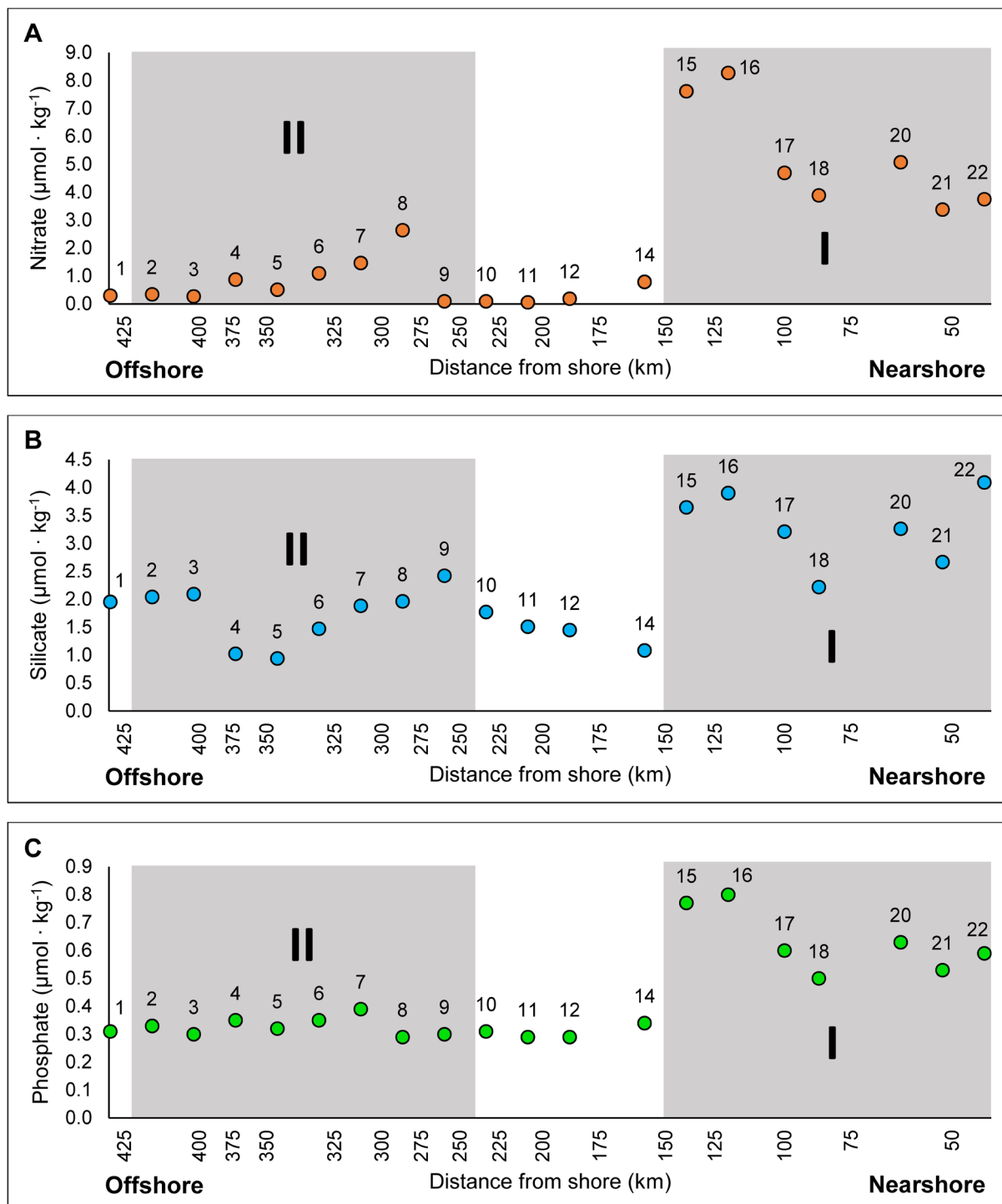
Figure 4. Measurements of surface macronutrient concentrations along the cruise track (**A**) nitrate, (**B**) silicate, and (**C**) phosphate. Grey boxes demarcate the boundaries of eddies I and II. The numbers above the datapoints represent the station number.

Dissolved Fe:Nitrate (dFe:Nitrate) ratio calculations (Figure 5A) ranged from 0.017 nmol/µmol at station 19 to 4.4 nmol/µmol at station 11. The dFe:Nitrate average in eddy I was 0.04 nmol/µmol ± 0.02 nmol/µmol, the eddy II average was 0.52 nmol/µmol ± 0.78 nmol/µmol, and the non-eddy average was 2.15 nmol/µmol ± 1.72 nmol/µmol. dFe:Nitrate was significantly different (Appendix Table 1C) across the three regions (eddy I, eddy II, and non-eddy), $H(2, 21) = 10.5$; p-value < 0.05. Post hoc tests reveal that the differences in dFe:Nitrate between eddies I and II and between eddy I and non-eddy were significant (p-values < 0.05; Appendix Table 2) while the difference between eddy II and non-eddy was not significant.

Silicate:Nitrate ratio calculations (Figure 5B) ranged from 0.47 at station 16 to 28.58 at station 11. The Silicate:Nitrate average in eddy I was $0.67 ± 0.2$, eddy II average was $5.70 ± 8.40$, and the non-eddy average was $12.54 ± 10.95$. Silicate:Nitrate was significantly different (Appendix Table 1C) across the three regions (eddy I, eddy II, and non-eddy), $H(2, 21) = 14.3$; p-value < 0.05. Post hoc tests reveal that the differences in Silicate:Nitrate between eddies I and II and between eddy I and non-eddy were significant (p-values < 0.01; Appendix Table 2) while the difference between eddy II and non-eddy was not significant.
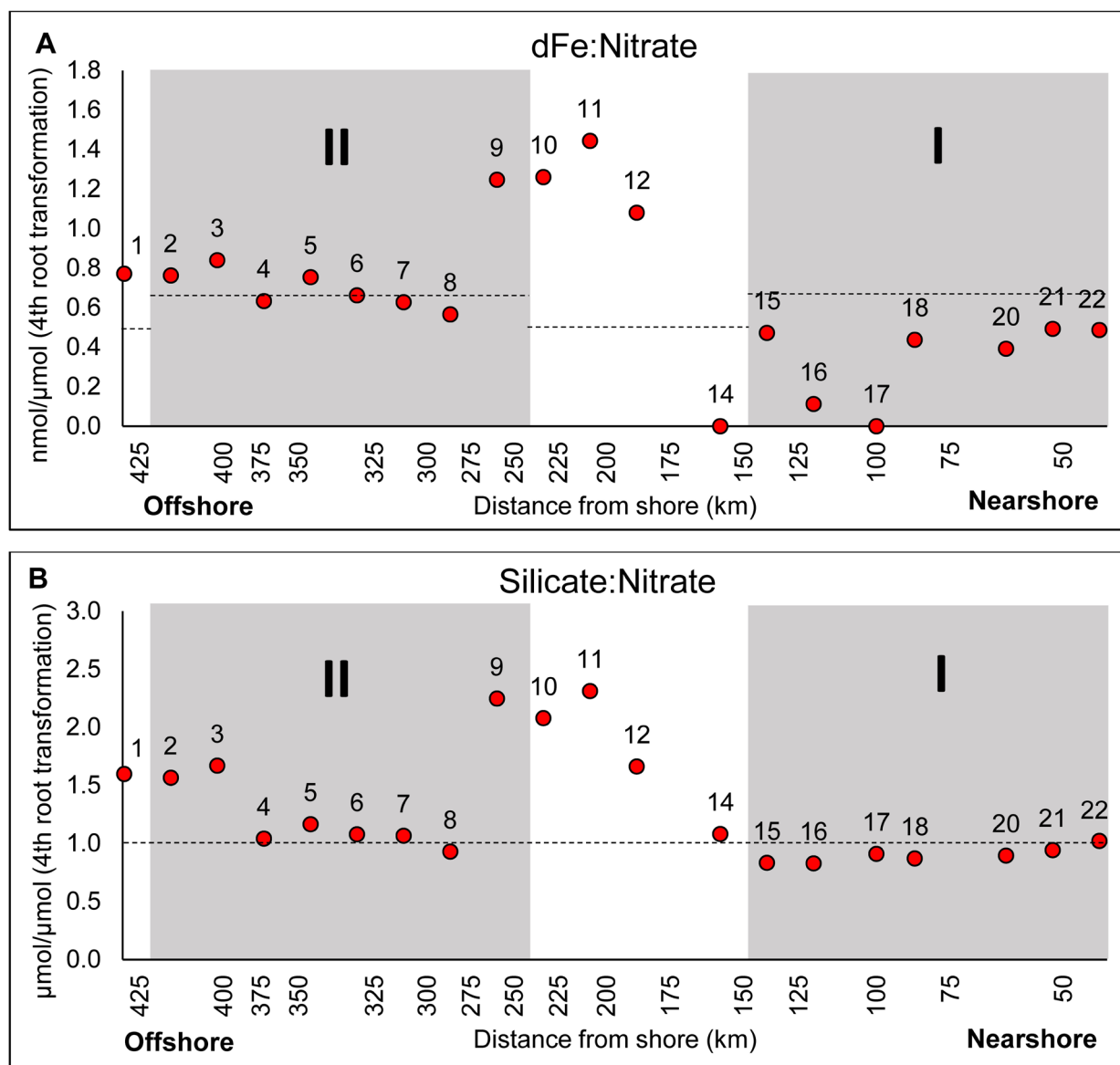
Figure 5. Ratios of (**A**) dFe:Nitrate and (**B**) Silicate:Nitrate. In plot A, the upper dashed line (0.67) differentiates nitrate limitation (above the dashed line) and Fe limitation (below) for coastal diatoms. The lower line (0.51) differentiates nitrate limitation (above) and Fe limitation (below) for oceanic diatoms. The dashed line in plot B (1.0) differentiates nitrate limitation (above) and silicate limitation (below). Grey boxes demarcate the boundaries of eddies I and II. The numbers above the datapoints represent the station number.

SPECIES DIVERSITY

Diversity (Figure 6A) and richness (Figure 6B) calculations were based on diatom OTU counts for each station. Eddy I and non-eddy stations were elevated in average diversity (3.0 ± 0.2 and 2.8 ± 0.1, respectively) while eddy II was characterized by lower average diversity, 1.8 ± 0.7. Diversity was significantly different (Appendix Table 1C) across the three regions (eddy I, eddy II, and non-eddy), $H(2, 20) = 10.4$; p-value < 0.05. Post hoc tests reveal that the differences in diversity between eddies I and II and between eddy I and non-eddy were not significant while the difference between eddy II and non-eddy was significant (p-values < 0.01; Appendix Table 2). Richness was not significantly different (Appendix Table 1B) across the three regions, $F(2, 17) = 2.1$; p-value $= 0.16$, nor were there significant differences in richness between any two regions (p-values > 0.05; Appendix Table 2). The relative abundance of *Rhizosolenia sp. 1* among diatom communities varied 11-fold across the transect (Figure 6C), ranging from $> 71\%$ of the community at stations 3, 6, and 7 to $< 0.01\%$ at station 20 (Appendix Table 4). There was a twenty-fold increase in *Rhizosolenia sp. 1* relative abundance across the front of eddy II, between stations 1 and 2. The average relative abundance of *Rhizosolenia sp. 1* in eddy I was 0.05 ± 0.08, non-eddy was 0.09 ± 0.05, and eddy II was 0.56 ± 0.20. Outside of eddy II, the highest abundance of *Rhizosolenia sp. 1* was at station 22 (Appendix Table 4). The relative abundance of *Rhizosolenia sp. 1* was significantly different (Appendix Table 1B) across the three regions (eddy I, eddy II, and non-eddy), $F(2, 17) = 31.5$; p-value < 0.05. Post hoc tests reveal that the differences in *Rhizosolenia sp. 1* relative abundance between eddies I and II and between eddy II and non-eddy were significant (p-values < 0.01; Appendix Table 2) while the difference between eddy I and non-eddy was not significant.
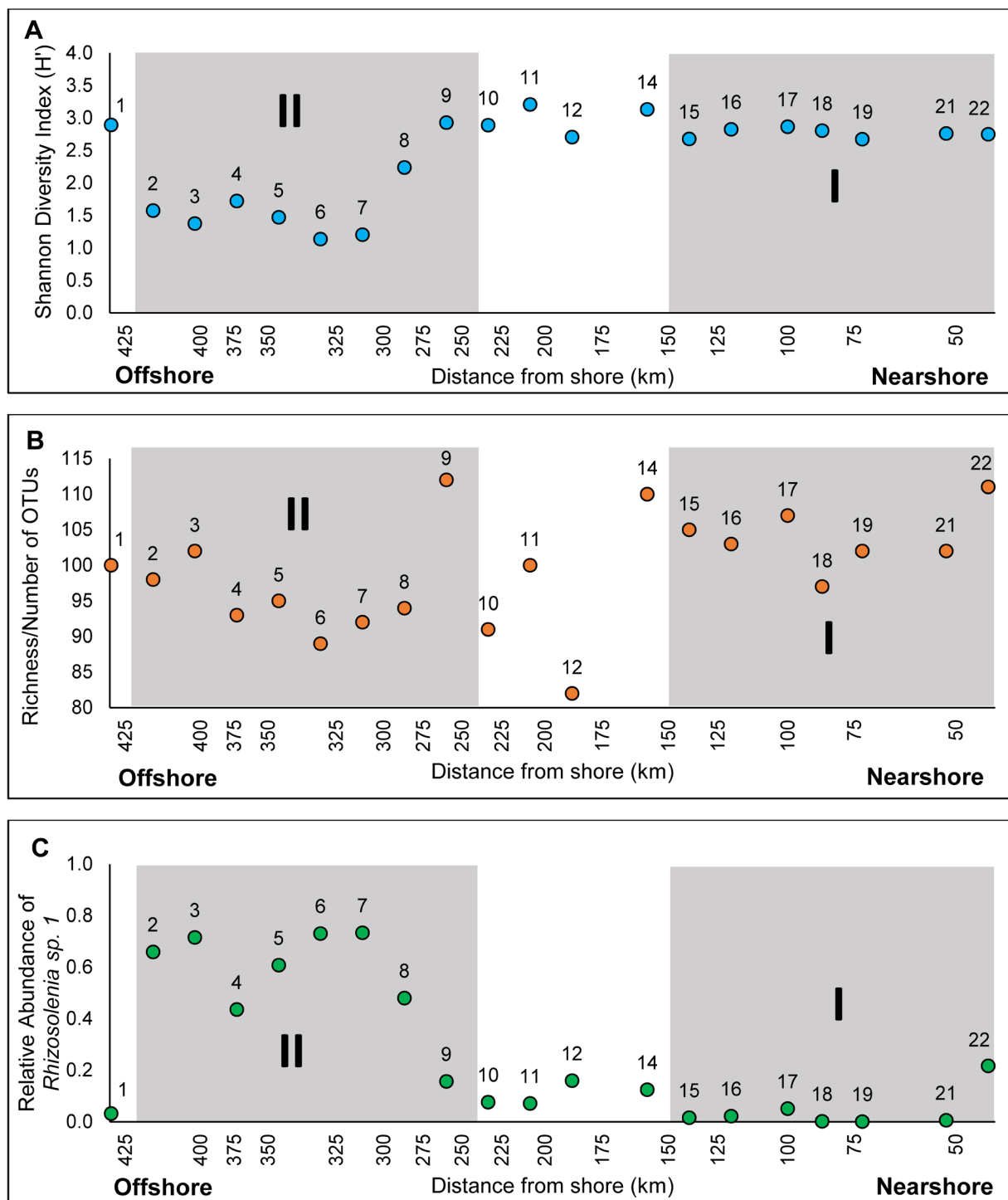
Figure 6. (**A**) Shannon diversity index (H'), (**B**) richness, and (**C**) relative abundance of *Rhizosolenia sp. 1*. Grey boxes demarcate the boundaries of eddies I and II. The numbers above the datapoints represent the station number.

DIATOM COMMUNITY COMPOSITION

The Bray-Curtis similarity dendrogram (Figure 7A) and community composition columns (Figure 7B) reveal the relatedness of stations based on their diatom community composition. While stations in eddy I clustered with similarity above 80%, eddy II did not exclusively cluster together. Stations 8 and 9 were part of eddy II based on the temperature and salinity graphs (Figure 2A-B) but clustered loosely with non-eddy rather than the rest of eddy II. Overall, there was lower similarity in the diatom community composition among the non-eddy stations.

The OTU with the highest read count, dominated the reads from the eddy II stations, was most similar in sequence to that of *Rhizosolenia shubsholei*, however, the sequence match between this OTU and *R. shubsholei* was only 91% (Appendix Table 3). For this reason, I have only classified this sequence to the genus level and refer to it as *Rhizosolenia sp. 1*. This lower match percentage classification was also given to three other OTUs, *Rhizosolenia sp. 2, Rhizosolenia sp. 3,* and *Thalassiothrix sp. 1*. The top 5 species in abundance along the transect (based on read counts) were *Rhizosolenia sp. 1, Fragilariopsis cf. kerguelensis, Actinocyclus sp. MPA-2013, Asteromphalus sp. TN-2014,* and *Pseudo-nitzschia cf. sp. A3ni*. Along with the three species of the *Rhizosolenia* (*R. sp. 1, R. sp. 2, R. sp. 3*), five different species of the genus *Pseudo-nitzschia* (*P. cf. sp. A3ni, P. americana, P. sp. A3ni, P. subcurvata,* and *P. delicatissima*) and three species of the genus *Thalassiosira* (*T. oestrupii*, *T. oceanica*, and *T. rischeri*) ranked among the top 20 OTUs in abundance. Detailed sequencing information including OTU names from NCBI, accession numbers, match percentage, and total reads for the top 20 OTUs are provided in Appendix Table 3. All remaining OTUs were grouped together in the "other identified species" category.
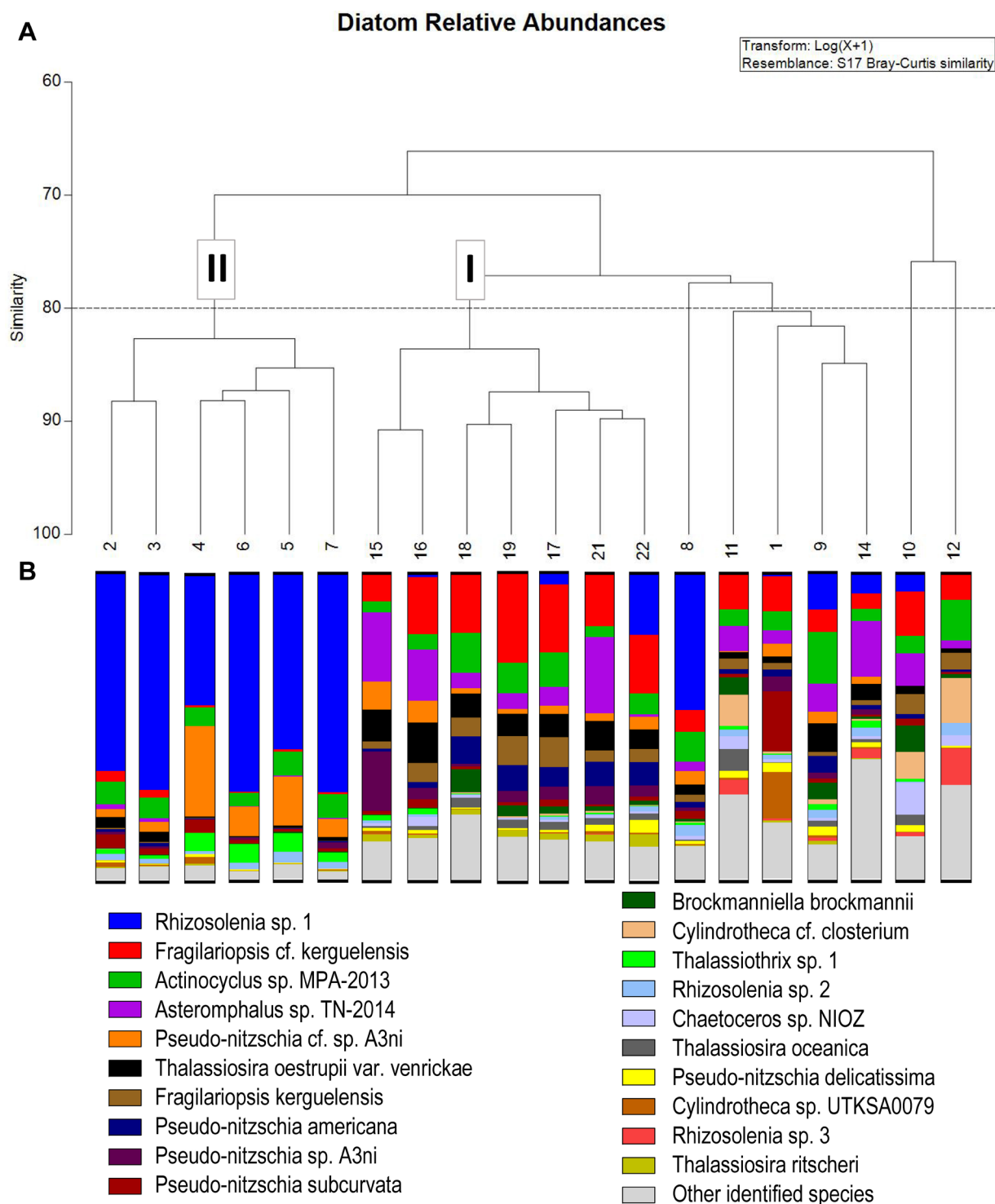
Figure 7. Diatom community structure. (**A**) Similarity dendrogram based on the group averages of the calculated Bray-Curtis values using PRIMER 7. A horizontal line indicates 80% similarity. Eddies I and II are indicated. (**B**) Composition columns of the diatom communities are shown below each corresponding station number. The colors within each column represent the species listed in the legend.

Line graphs of the relative abundance of the top 20 OTUs as they varied across the transect were categorized into one of six patterns. These classifications were based on the OTU's dominant pattern, noting that an OTU may also fit into other patterns. The one exception to this was the OTU classified as *T. oestrupii*, which was categorized into two different patterns. OTUs in pattern 1 (Figure 8) had a dramatic decrease in abundance from station 1 to 2. The two OTUs in pattern 1 were *P. subcurvata* and *Cylindrotheca sp. UTKSA0079.* OTUs in pattern 2 (Figure 9) had an elevated relative abundance in eddy II. The OTUs whose dominant pattern was type 2 were *Rhizosolenia sp. 1*, *Pseudo-nitzschia cf. sp. A3ni*, *Thalassiothrix sp. 1*, and *Rhizosolenia sp. 2*. Pattern 3 (Figure 10) OTUs had an elevated relative abundance in the stations between the two eddies. Pattern 3 was represented by four OTUs classified as: *Chaetoceros sp. NIOZ*, *Thalassiosira oceanica*, *Cylindrotheca cf. closterium*, and *Rhizosolenia sp. 3*. Pattern 4 (Figure 11) OTUs had an elevated relative abundance in eddy I. Pattern 4 OTUs included *Pseudo-nitzschia sp. A3ni*, *Fragilariopsis cf. kerguelensis*, *Fragilariopsis kerguelensis*, and *Thalassiosira ritscheri*. OTUs in pattern 5 (Figure 12) showed an overall elevated relative abundance in eddy I with a dip in relative abundance in the center stations of eddy I. Pattern 5 was represented by OTUs classified as *Asteromphalus sp. TN-2014* and *T. oestrupii*. Pattern 6 OTUs (Figure 13) had an elevated relative abundance in both eddy I and the trailing edge of eddy II. This pattern was represented by OTUs classified as *Actinocyclus sp. MPA-2013*, *T. oestrupii*, *P. americana*, *Brockmanniella brockmannii*, and *P. delicatissima*.
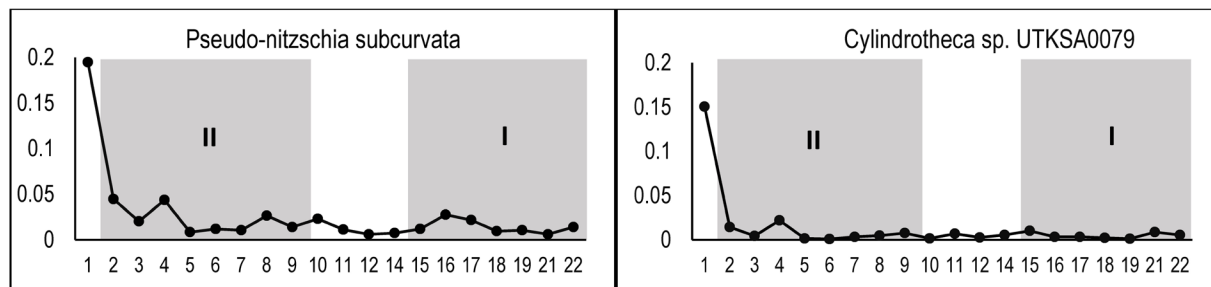
Figure 8. Pattern 1: Sharp decrease in relative abundance from Station 1 to Station 2.
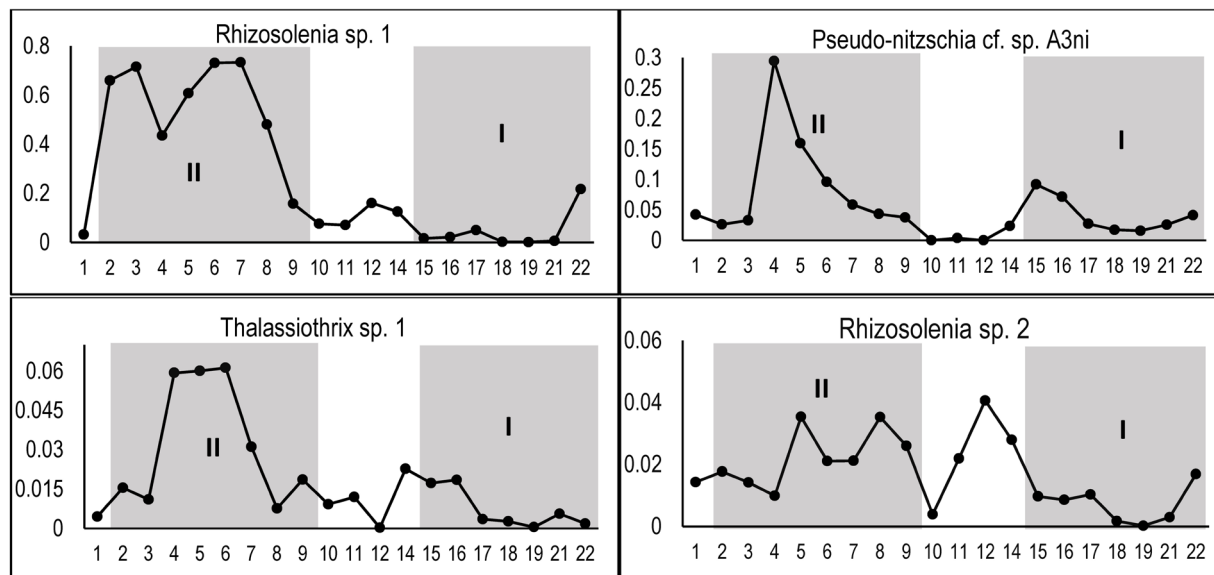
Figure 9. Pattern 2: Elevated relative abundance in eddy II.
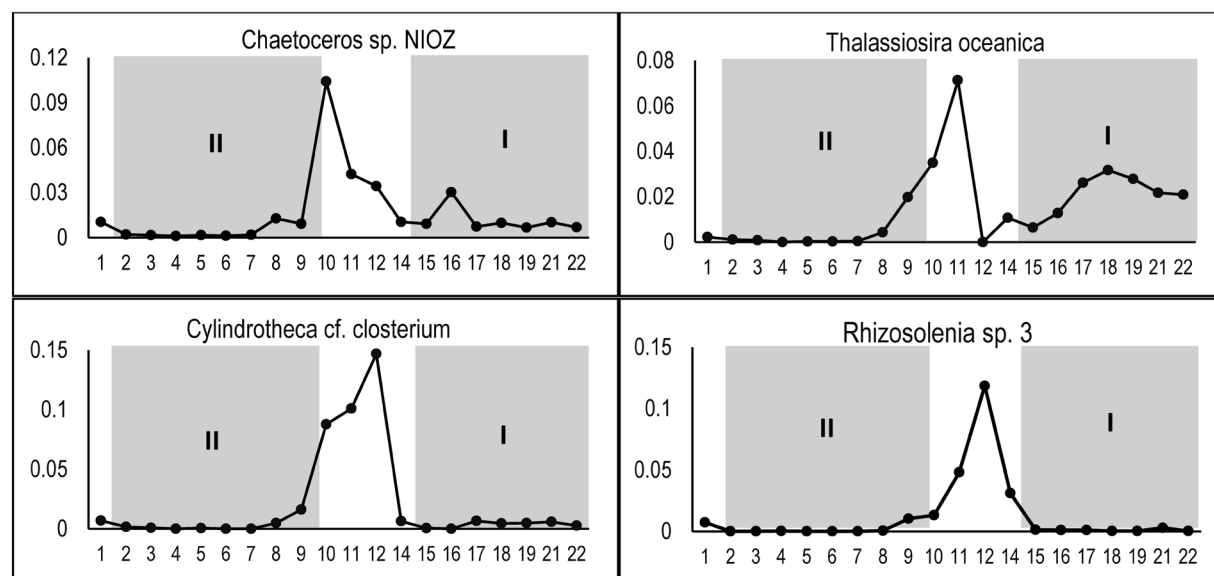
Figure 10. Pattern 3: Elevated relative abundance in between eddies (Stations 10-14).
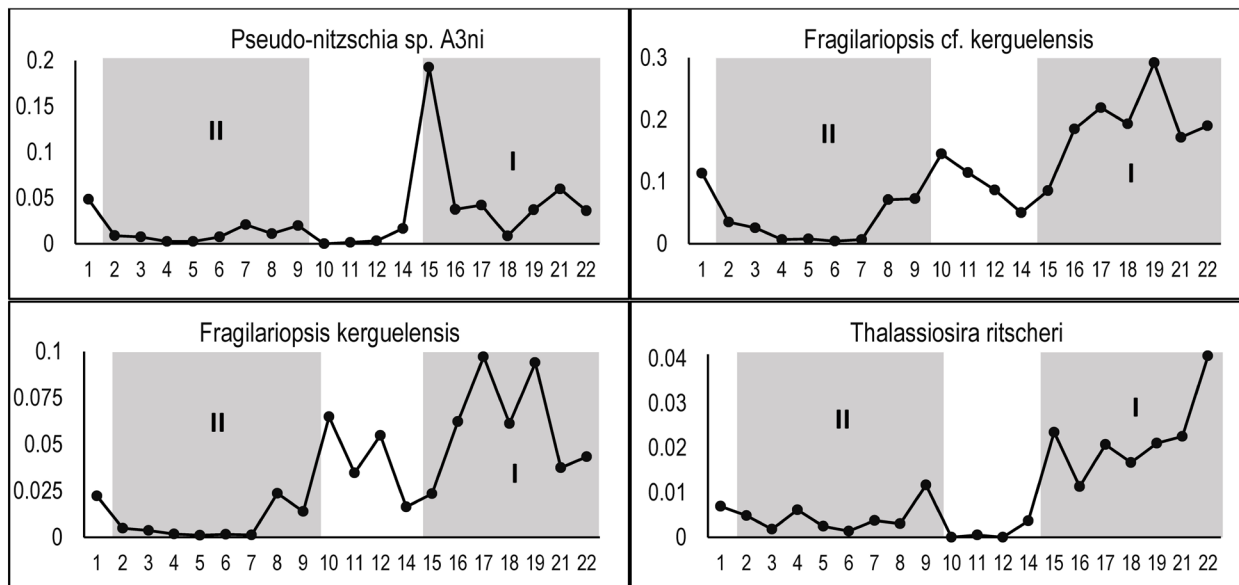
Figure 11. Pattern 4: Elevated relative abundance in eddy I.
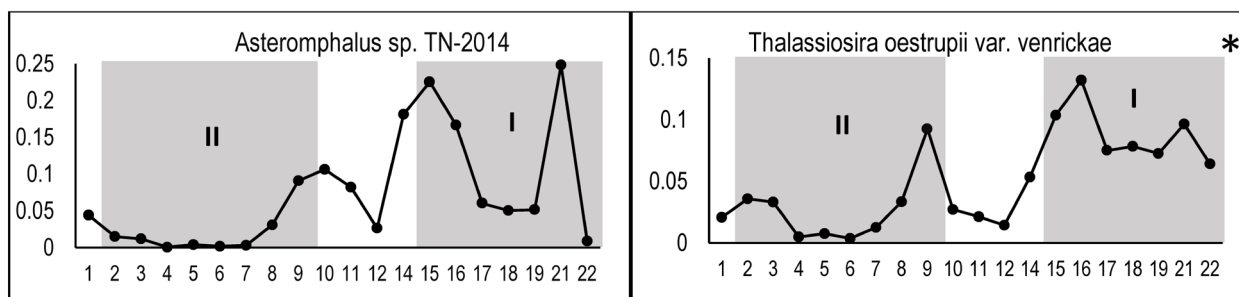
Figure 12. Pattern 5: Elevated relative abundance in eddy I with lower relative abundance in the center (Stations 17-19). *Thalassiosira oestrupii var. venrickae* is also categorized in pattern 6.
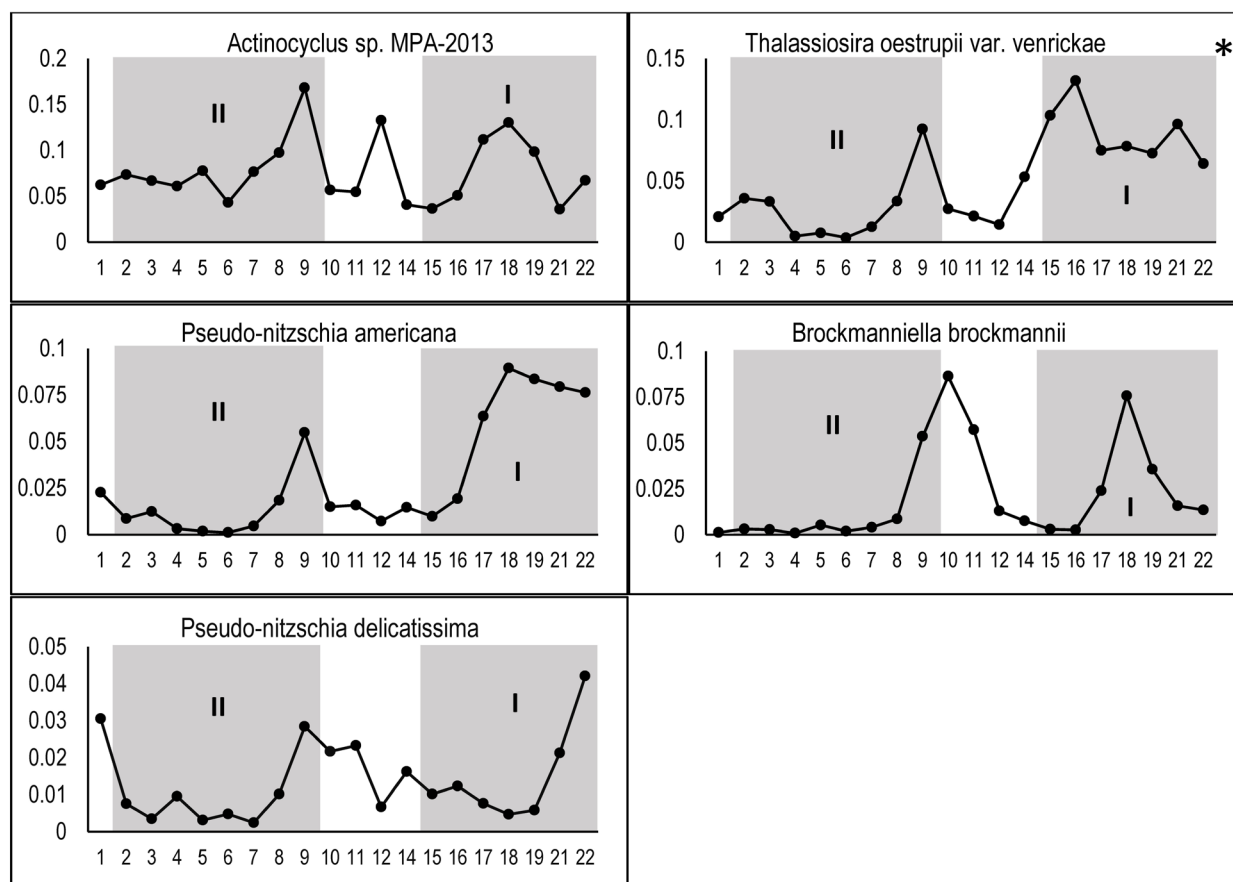
Figure 13. Pattern 6. Elevated relative abundance in both eddy I and trailing edge of eddy II.
Thalassiosira oestrupii var. venrickae is also categorized in pattern 5.

We note that the region amplified by our primers are not diagnostic for *Fragilariopsis* species, with *F. kerguelensis, Fragilariopsis curta* and *Fragilariopsis sublineata* all identical in sequence in this region. These three *Fragilariopsis* species are all found in the Southern Ocean and have not been reported in the North Pacific Ocean. There is a *Fragilariopsis* species, *F. pseudonana*, that has been found to dominate the Eastern temperate zone of the North Pacific Ocean (Aizawa et al., 2005), but there is no 18S sequence data that covers the region amplified by our primers available for that species.

To quantify the impact of *Rhizosolenia sp. 1* relative abundance on the Shannon diversity index (H'), a linear regression was performed (Figure 14) and showed that the two variables have a significant negative correlation, $r = -0.9421$, *p*-value < 0.05. While the blue points (eddy II values) were mostly grouped on the right-hand side of the plot, there was one point (station 9) that was grouped with eddy I and non-eddy stations. Additionally, 6 of the 7 eddy I stations fall below the line of best fit, while 4 of the 5 non-eddy stations fall above the line.
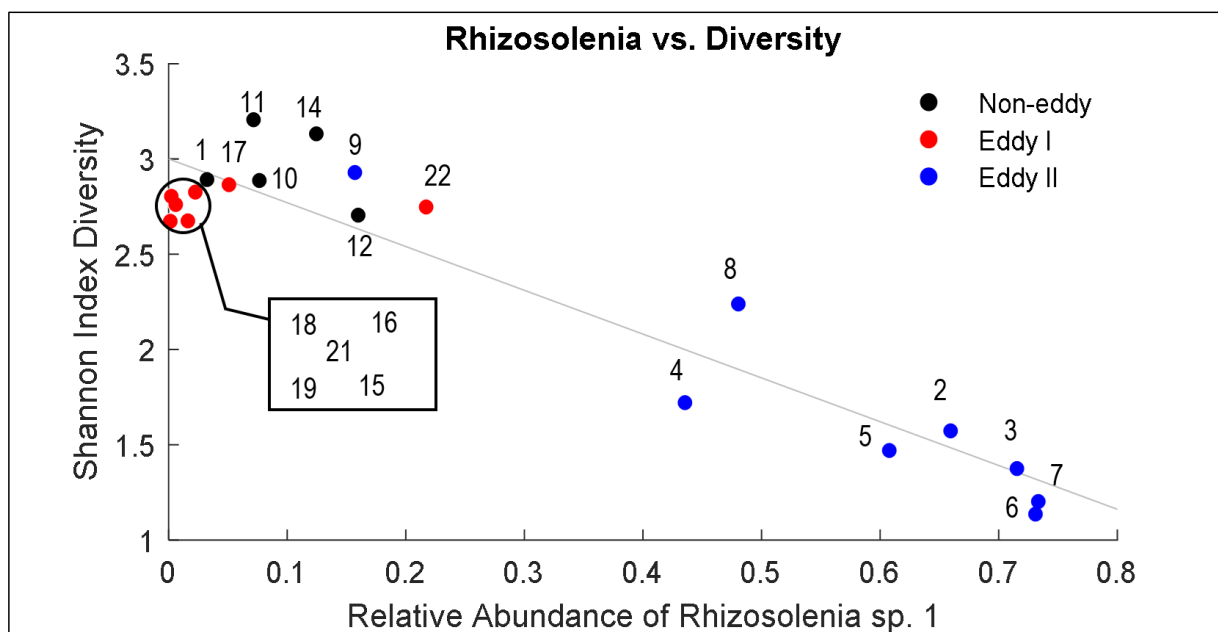
Figure 14. Scatterplot of *Rhizosolenia sp. 1* relative abundance and Shannon index diversity (H') calculations. A line of best fit has been added, represented by *y = −2.3x + 3.0*. The relative abundance of *Rhizosolenia sp. 1* and diversity have a significant negative correlation, $r = -0.9421$, $p < 0.05$.

DISCUSSION

The limited exchange of water across cyclonic eddy boundaries in the CCS creates natural mesocosms wherein the original coastal planktonic communities trapped in the eddy undergo ecological succession as the eddy ages and travels offshore. I sampled two eddies of different ages to approximate the time evolution of CCS eddies by comparing the biogeochemical and ecological characteristics. The biogeochemical properties of the three regions – eddies I, II, and non-eddy – uncovered the strong environmental differences among the regions. These differences were echoed in the distinct diatom community compositions, with the strongest community similarities seen within eddies I and II. Here, I discuss the physical (temperature, salinity, fluorescence, and density), biogeochemical (nutrient concentrations and limitations), and ecological (diatom community composition) differences among the three regions and the apparent drivers. Eddy II, hosting 10 months of a hotspot of ecological succession, was largely dominated by one diatom species within the genus *Rhizosolenia*. I discuss the adaptations of *Rhizosolenia*, evidence supporting the presence of a vertically migrating mat species of *Rhizosolenia*, stipulations to this study, and areas for future research.

EDDY I

The formation and development of cyclonic mesoscale eddies in the CCS have been studied and modeled in depth (Chenillat et al., 2018; Chenillat et al., 2016; Chenillat et al., 2015). The outermost concentric ring of an eddy is the youngest and latest addition and is composed of water from a variety of regions including recently upwelled waters (Chenillat et al., 2018), which creates a strong front on the western boundary of the eddy, especially in newly developed eddies. Dramatic shifts seen in the temperature (Figure 2A), salinity (Figure 2B), and nutrient concentrations (Figure

4) crossing from California Current water (station 14) into eddy I (station 15) can thus be attributed to newly upwelled waters having been recently wrapped around the eddy. Post hoc testing confirmed the strength of the front, as eddy I was significantly different in temperature, salinity, and all three macronutrients when compared to both eddy II and non-eddy (Appendix Table 2). Eddy I also showed a dip in salinity between stations 20-22, which could be attributed to a coastal upwelling filament (Marchesiello et al., 2003). The fluorescence measurements at stations 15 and 16 (taken at 7 pm and 8 pm PST, respectively) were surprisingly low for their macro-nutrient concentrations and were not significantly impacted by the non-photochemical quenching effect (Bilger, Schreiber, & Bock, 1995; Murchie & Lawson, 2013). Areas high in macro-nutrients and low in chlorophyll could signify a micro-nutrient limitation (Bruland et al., 2001; Falkowski et al., 1998) or a pre-bloom stage where the primary producers have just received nutrient delivery (Engel, Goldthwait, Passow, & Alldredge, 2002).

EDDY II

Eddy II had significantly higher temperatures than eddy I (Figure 2A), not surprising considering that these surface waters had been exposed to 10 months of solar radiation since separation from coastal upwelling influences. Eddy II experienced limited exchange with California Current waters during this time, reduced access to nutrient-rich coastal waters and sustained photosynthetic activity would have led to the observed depletion of nutrients (Figure 4). The salinity measurements of eddy II (Figure 2B) resembled a tiered structure and was fairly symmetrical. Stations 5-6 were the center of the eddy, with stations 4 and 7 as part of a concentric ring around stations 5-6. The next ring was composed of stations 2-3 on the western boundary (leading edge) and stations 8-9 on the eastern boundary (trailing edge). There was a significant drop in

temperature and a slight increase in salinity in eddy II between stations 8-9, which could have been a signature of localized, small-scale upwelling or coastal filament, either of which could explain the increase in fluorescence and nitrate in the same region. This effect may also be a product of eddy leakage, a process that has been documented in the later stages of the eddy's life (Chenillat et al., 2018). The fluorescence inside eddy II was much higher than at station 1, outside it to the southwest. Note that because station 1 was sampled at midnight, the lower fluorescence was not the result of non-photochemical quenching.

DIATOM COMMUNITIES

Diatom community shifts can reveal relationships between diatoms and their environment, which can include those induced by both physical and biogeochemical factors. In this study, the eddies exhibited communities genetically distinct from one another, both of which differed from the community in the non-eddy areas. I also observed distinct differences in environmental conditions explicable by our understanding of the nature of eddy formation and dynamics. Eddies in the CCS have high nonlinearity, which limits the exchange with surrounding waters (Chenillat et al., 2018). This partial isolation of CCS eddies allows for nutrient drawdown and ecological succession of diatoms. The concentric ring structure and formation of these eddies is reflected in the Bray-Curtis similarity dendrogram of the diatom communities (Figure 7). In eddy I, stations 15 and 16 grouped together and originated from the most recently upwelled waters. Stations 17-19 grouped together and were part of the original parcel of water trapped by the eddy that has undergone a two-month succession since formation. Stations 21 and 22 grouped together apart from 17-19. While the surface waters of these 5 stations all originated from the same region where the eddy formed,

stations 21 and 22 were located above the continental shelf, thus they remain in close proximity to upwelling, mixing, and runoff from the coast.

The community dendrogram structure of eddy II was similar to that of eddy I, despite the differences in age and composition. Stations 2 and 3 grouped closely each other and with other eddy II stations but remained distinct from stations 4-7 in the eddy center. Stations 8 and 9 were part of the trailing edge of eddy II and the communities were more similar to non-eddy stations than any other eddy II stations. This result may have been linked to the unusual characteristics of the region between stations 8 and 9, where there was a significant drop in temperature, slight increase in salinity, a surge in both fluorescence and nitrate, and the highest community diversity and richness of all eddy II stations. Finally, while there was less similarity among the non-eddy stations compared to the similarity within each eddy, the non-eddy stations grouped according to similar sea surface heights. This clustering signifies that many of the diatoms inside parcels of water along the same sea surface heights once occupied the same space.

EFFECT OF NUTRIENT LIMITATION ON DIATOM COMMUNITIES

Nutrient limitation calculations for Fe:Nitrate and Silicate:Nitrate were in performed in accordance with previous studies (Biller & Bruland, 2014; Brzezinski, 1985) to compare the nutrient concentrations to diatom nutrient requirements for growth. Eddy I was high in macronutrients and although nutrient ratios suggest Fe and silicate limitation (Figure 5), there were still sufficient nutrients to support a diverse community of coastal diatoms known to have higher nutrient requirements. The broad shelf area off Cape Mendocino has previously been described as an Fe-replete region (Bruland et al., 2001). Discovering Fe-limitation in a normally Fe-replete region was also discovered during the same cruise in a shelf region off Cape Blanco, Oregon, just 300 km

north (Till et al., 2019). If Fe-limitation has become more common in coastal regions than previously thought, it could have a significant impact on coastal productivity, carbon exchange, and carbon export estimates, especially considering the NE Pacific is a diatom-dominated region (Wilson et al., 2008). Silicate is also not a typical limiting nutrient in the NE Pacific (Wilson & Qiu, 2008), but eddy I was limited by silicate. Since sampling took place in the mid- to late upwelling season, this silicate limitation may have been an artifact of earlier diatom blooms that drew down silicate in surface waters. Nutrient ratios in eddy II, on the other hand, suggest phytoplankton growth was limited by nitrate, which could have resulted from nutrient depletion by phytoplankton activity over the 10 months since eddy formation. Looking at Silicate:Nitrate ratios, eddy II was limited by nitrate at 7 of 8 stations. Examining Fe:Nitrate ratios and assuming the eddy II diatom communities were of coastal origin, eddy II was limited by nitrate for half the stations (2-3, 5, 9) and limited by Fe for the other half (4, 6-7).

The depleted nitrate concentrations at the surface of eddy II mimics oligotrophic conditions and appears to have influenced the diatom community. *Rhizosolenia*, a genus of morphologically large diatoms with high silicate requirements known to have strategies to bypass nitrate limitation (Villareal, Woods, Moore, & CulverRymsza, 1996), was by far the most abundant diatom sequence recovered in this study. The diversity of eddy II was largely driven by the relative abundance of a single *Rhizosolenia* species (Figure 14). *Rhizosolenia sp. 1* accounted for over 40% of the diatom community in 7 of 8 eddy II stations with sequences at 3 of these stations being composed of over 70% *Rhizosolenia sp. 1*. According to post hoc testing, eddy II was significantly different in *Rhizosolenia sp. 1* relative abundance compared to both eddy I and non-eddy (Appendix Table 2). One species of this genus of diatom was dominant in the community at the nitrate-limited stations 2 and 3 but decreased in relative abundance by more than 40% at the low-

silicate, Fe-limited station 4. There, with both nitrate and silicate concentrations approximately1 µmol/kg, *Rhizosolenia sp. 1* may have experienced co-limitation and transitioned to a senescent stage, allowing other diatoms to increase in abundance. It is also worth noting that the highest silicate concentration along the transect was at station 22, also where this species of *Rhizosolenia* exhibited highest abundance outside eddy II.

Rhizosolenia sp. 2 was also a notable presence in eddy II (Figure 9), mirroring the general structure of *Rhizosolenia sp. 1*, including elevated relative abundance in eddy II and an increase in abundance at station 22. Additionally, *Rhizosolenia sp. 1* showed a slight increase in relative abundance in between the eddies at station 12, where the relative abundance of *Rhizosolenia sp. 2* was at its highest. Two *Rhizosolenia* species that were not in the 20 most abundant taxa, *R. formosa* and *R. delicatula*, also had elevated relative abundances between eddies, with their highest abundances at station 12 and 14, respectively (Appendix Figure 3).

RHIZOSOLENIA TRAITS

One of the advantageous traits of the *Rhizosolenia* genus is the ability of cells to congregate into mats and regulate buoyancy to migrate vertically and access deep nitrate pools. The buoyancy mechanism is regulated by ballasting from changes in carbohydrate concentration within the cell via carbohydrate production and consumption (Letscher & Villareal, 2018; Villareal et al., 1996). Carbohydrates accumulate within *Rhizosolenia* mats at the surface during photosynthesis, then are consumed at depth for respiration and for nitrate uptake, which then de-ballasts the cell (Singler & Villareal, 2005). One study has confirmed via isotopic and optical methods that *Rhizosolenia* access nitrate from below the euphotic zone (Villareal, Pilskaln, Montoya, & Dennett, 2014) up to 305 m below the surface (Pilskaln, Villareal, Dennett, Darkangelo-Wood, & Meadows, 2005).

Vertical migration of *Rhizosolenia* mats has been characterized as an asynchronous, non-diurnal migration (Villareal et al., 1996). When *Rhizosolenia* mats migrate vertically, they access new nitrate below the euphotic zone and return to the surface to carry out photosynthesis on a large scale, removing substantial amounts of carbon from surface waters more efficiently than non-vertically migrating phytoplankton (Wilson & Qiu, 2008). This phenomenon is in contrast to upwelling events, which in addition to supplying nitrate to the surface, translocates carbon as well, which lowers the carbon concentration gradient at the air-sea interface (Wilson & Qiu, 2008). Therefore, a significant presence of *Rhizosolenia* mats in CCS eddy diatom communities can greatly impact the carbon cycling and export estimates. Mat accumulation at the surface occurs for several days at a time (Richardson, Cullen, Kelley, & Lewis, 1998), especially during low-wind periods (Villareal et al., 1996). Eight species have been identified in mats in the NE Pacific, including *R. castracanei, R. debyana, R. acuminata, R. formosa, R. ostenfeldii, R. decipiens, R. fallax* (Alldredge & Silver, 1982; Carpenter, 1977; Martínez, Silver, King, & Alldredge, 1983; Venrick, 1971; Villareal, 1987; Villareal & Carpenter, 1989) and *R. imbricata var. shrubsolei* (Alldredge & Silver, 1982). One of these studies found that *R. fallax* was present in all the mats they sampled, suggesting that it acted as a "matrix" for mat formation (Villareal & Carpenter, 1989). It is important to note, however, that the majority of the *Rhizosolenia* species previously identified as mat formers are not present in the Bacillariophyta group of the NCBI 18S library of sequences, including *R. castracanei, R. debyana, R. acuminata, R. ostenfeldii,* and *R. decipiens*. The absence of these 18S sequences could explain why the match percentages of our *Rhizosolenia* species 18S sequences to the library *Rhizosolenia shubsholei* 18S sequence were quite low at 91% (*R. sp. 1*), 92.7% (*R. sp. 2*), and 94.1% (*R. sp. 3*) (Appendix Table 3). Further, the full NCBI 18S sequence of *R. fallax* is a 100% match to that of *R. formosa*, meaning the *R. formosa* detected in

our sampling with elevated relative abundance in between the eddies (Appendix Figure 3) could just as likely be *R. fallax*.

In addition to buoyancy regulation, some *Rhizosolenia* are also known to host the cyanobacterium *Richelia intracellularis* as an endosymbiont in a diatom-diazotroph assemblage (DDA) (Villareal, Adornato, Wilson, & Schoenbaechler, 2011). *R. intracellularis* fixes dinitrogen (N_2) into a bioavailable form of nitrogen to fulfill the nitrogen requirements of itself and the host diatom; as much as 97.3% of the total fixed N_2 goes to the diatom (Foster et al., 2011). Thus far, *R. clevei* is the only *Rhizosolenia* species that has been identified in CCS *Rhizosolenia-Richelia* DDAs (Kemp & Villareal, 2013; Villareal et al., 2011; Villareal & Carpenter, 1989) that is not present in the Bacillariophyta group of the NCBI 18S library of sequences.

EVIDENCE FOR VERTICALLY MIGRATING MATS

While the *Rhizosolenia* sequences that were categorized as top 20 OTUs cannot 100% be confirmed as one of the vertically migrating, mat-forming species or the DDA species, our results provide more evidence supporting *R. sp. 1* and *R. sp. 2* function as part of vertically migrating mats. Firstly, the top hit for both OTUs were *R. shrubsolei* (Appendix Table 3), a known mat-forming species (Villareal, 1987). Because there are two species of *Rhizosolenia* with elevated relative abundances present in eddy II, it is possible that they formed multi-species mats as found in previous studies (Villareal & Carpenter, 1989). Also, the low wind speed conditions (hovering between 8-12 m/s) in eddy II (Appendix Figure 1) would be suitable, though near the upper limit, for *Rhizosolenia* mats to remain intact (Richardson et al., 1998; Villareal & Carpenter, 1989; Villareal et al., 1996). Additionally, the process of N_2 fixation for diazotrophs is energetically expensive and dependent on sufficient Fe bioavailability (Falkowski et al., 1998; Mellett et al.,

2018) for nitrogenase to function properly (Wilson & Qiu, 2008). Based on the magnitude of the *Rhizosolenia* dominance, we might expect to see Fe limitation in eddy II if N_2 fixation was occurring on such a large scale. Instead, I found that while eddy II had low Fe, Nitrate was near depletion and the limiting nutrient of eddy II.

Assuming the *Rhizosolenia* in eddy II were vertically migrating mats, they were likely Fe-stressed based on a previous study that found Fe-stress to be associated with low F_v/F_m values (Appendix Figure 2) in *Rhizosolenia* mats (Singler & Villareal, 2005). Also, because *R. formosa*, observed in low relative abundance between eddies, is a known species in vertically migrating mats (Richardson, Ciotti, Cullen, & Villareal, 1996; Villareal, 1987), there may have been vertically migrating mats in between the eddies, but in much lower relative abundance.

IMPACT OF OUR RESULTS ON THE SCIENTIFIC COMMUNITY

Our results suggest that cyclonic eddies do more than just trap coastal waters and sustain high productivity as they age and travel offshore. Ecological succession of the eddies' constituent biological communities is also an important factor to consider. As our results have shown, diatom community composition can shift in response to both physical processes inherent to eddies and to a depletion of nutrients by coastal diatoms. Incorporation of ecological succession in studies of biophysical interactions of eddies can greatly impact carbon cycling and carbon export estimates as well as the estimate of total nitrate transported by eddies across the CCS. A recent model suggests that CCS cyclonic eddies are responsible for 50% of lateral transport of nitrate offshore (Chenillat et al., 2016), which may be an overestimation considering the average nitrate concentration of eddy II was 0.82 μmol/kg. Additionally, while there may be elevated biological activity in a cyclonic eddy for a period of time, the biological activity will plateau at some point

because of the nutrient drawdown from coastal communities. By the time an eddy dissipates offshore, the phytoplankton communities will be quite different from the communities trapped during the eddy's formation.

It is important to address the seasonality of phytoplankton communities in the CCS region (Du & Peterson, 2013) and the impact that season-to-season shifts in community could have had on my results. Eddy I formed 2 months prior to sampling around mid-May and just after the start of the coastal upwelling in the Northern California region (Lassiter, Wilkerson, Dugdale, & Hogue, 2006) while eddy II formed 10 months prior to sampling around mid-September. Studies have previously found that phytoplankton (and diatom) communities undergo seasonal shifts in composition (Du & Peterson, 2013; Peterson et al., 2017; Sancetta, 1995). A study in the upwelling region off the coast of Northern California's Bodega Bay found nearly identical coastal diatom communities in the same location in yearly intervals in the mid-May to late-June timeframe, with elevated relative abundances of *Chaetoceros* and *Rhizosolenia*, though the *Rhizosolenia* species switched from *R. delicatula* in 2001 to *R. setigera* in 2002 (Lassiter et al., 2006). In this shelf region, despite high turbulence and mixing, the diatom community composition remains relatively consistent year-to-year, suggested to be caused by a benthic resting stage by these recurrent species (Lassiter et al., 2006). A study off the coast of Cape Mendocino in mid-June of 1987 found *R. alata* in elevated relative abundances, along with species of *Chaetoceros* and *Thalassiosira* (Hood et al., 1990). Because of these previous findings, seasonality could have been a significant driver in the stark difference in diatom communities between eddies I and II. However, the role of seasonality in my study remains undetermined, as there were no samples obtained at the time of eddy formation for either eddy.

Additionally, the inclusion of samples from a range of depths would have assisted in creating a more complete assessment of the ecological and biogeochemical dynamics of the eddies. Using the same sequencing methods for obtaining the surface diatom community composition at different depths would uncover whether the *Rhizosolenia* species in my study were migrating vertically, which is an important distinction for this study. The physical and chemical properties and community compositions at depth would also be informative for the areas along the transect that showed unusual fluctuations in these properties at the surface. There are both advantages and drawbacks with implementing a study that only uses surface samples. Surface-only experiments allow for faster sampling which provides a nearly true snapshot of the region. They are also less expensive in terms of ship time, extraction materials, and sequencing costs. Experiments with depth profiles, however, provide more comprehensive and conclusive results.

FUTURE RESEARCH

This study provides valuable insight into the impact of mesoscale cyclonic eddy dynamics on diatom communities in the CCS. In the future, a series of incubation experiments tracking the ecological succession of coastal diatoms (+/- *Rhizosolenia* additions) under both coastal and oligotrophic nutrient conditions would be helpful in understanding the fine-scale biological activities occurring during the ecological succession. The samples from this study could also be tested for the presence of N_2 fixation via *nif* gene expression to more definitively classify the *Rhizosolenia* collected. Additional studies involving long-term, Lagrangian sampling of eddies are needed to provide a more comprehensive view of biological activity in CCS eddies. This type of process has previously been performed utilizing an aquatic autonomous vehicle that has captured data on optics, imaging, and photosynthetic efficiency of diatom blooms in the NE Pacific

(Anderson, Wilson, Knap, & Villareal, 2018). The Anderson et al. (2018) study could be used as a model for gathering similar data within an eddy as it ages and travels offshore. Finally, the estimates for carbon cycling and export in the region should be revisited to account for *Rhizosolenia* mats. The effect of *Rhizosolenia* mats on carbon cycling has a stronger impact by biomass on the removal of CO_2 from the atmosphere compared to coastal upwelling-fueled diatom blooms (Wilson & Qiu, 2008), making an important contribution to minimizing the impacts of CO_2 emissions that influence climate change. The estimate of nitrate transport in the CCS via mesoscale cyclonic eddies should also be adjusted to factor in the drawdown of nutrients by phytoplankton during eddy development.

CONCLUSION

The high nonlinearity of CCS mesoscale cyclonic eddies impacts diatom communities by limiting their interaction with surrounding waters, leading to ecological succession. Our results suggest that both the biogeochemistry and diatom community structure within cyclonic eddies evolve as the eddies move offshore from the coast. The high-nutrient, high-diversity coastal waters are initially dominated by coastal diatoms known to have higher nutrient requirements. As the nutrients within the eddy are drawn down over time, species equipped with low-nutrient adaptations can become dominant and affect diversity. The combined effect of transport by, and ecological succession within the eddies is likely a key factor in mediating carbon cycling and export across the wider CCS region.

APPENDIX

Appendix Table 1A. Tests for Normal Distribution for Select Variables						
	Temperature	Salinity	Fluorescence	Nitrate	Silicate	Phosphate
Skewness	-0.43	-0.63	0.27	0.95	0.64	0.97
Kurtosis	-1.38	-0.98	-0.69	-0.17	-0.41	-0.27
KS stat (*D*)	0.23	0.19	0.13	0.22	0.13	0.27
***p*-value**	0.18	0.38	0.79	0.21	0.82	0.08
Normal?	normal	normal	normal	normal	normal	normal

	Silicate:Nitrate	Fe:Nitrate	Diversity (H')	Rhizosolenia Rel. Abun.	Wind Speed	Density	Richness
Skewness	2.01	2.39	-0.80	0.73	0.50	0.26	-0.24
Kurtosis	3.12	5.49	-1.02	-1.24	-1.22	-1.44	-0.19
KS stat (*D*)	0.34	0.36	0.31	0.25	0.19	0.22	0.09
***p*-value**	0.01	0.007	0.03	0.14	0.41	0.22	0.99
Normal?	not normal	not normal	not normal	normal	normal	normal	normal

Appendix Table 1B. One-way ANOVA (Analysis of Variance) Results
Groups defined as eddy I, eddy II, and non-eddy

Variables	Between Groups *df*	Within Groups *df*	*F*-statistic (distance between groups)	*p*-value	Significant?
Temperature	2	18	45.1	$p < 0.05$ ($9.8 \, e^{-8}$)	Yes
Salinity	2	18	40.1	$p < 0.05$ ($2.3 \, e^{-7}$)	Yes
Fluorescence	2	18	8.1	$p < 0.05$ (0.003)	Yes
Nitrate	2	18	38.3	$p < 0.05$ ($3.3 \, e^{-7}$)	Yes
Silicate	2	18	17.1	$p < 0.05$ ($6.9 \, e^{-5}$)	Yes
Phosphate	2	18	47.1	$p < 0.05$ ($6.9 \, e^{-8}$)	Yes
Rhizosolenia Relative Abundance	2	17	31.5	$p < 0.05$ ($1.9 \, e^{-6}$)	Yes
Wind Speed	2	18	40.1	$p < 0.05$ ($2.3 \, e^{-7}$)	Yes
Density	2	18	85.3	$p < 0.05$ ($6.6 \, e^{-10}$)	Yes
Richness	2	17	2.1	$p = 0.16$	No

Appendix Table 1C. Kruskal-Wallis Test Results for non-normal data
Groups defined as eddy I, eddy II, and non-eddy

Variables	Between Groups *df*	Number of Observations (*N*)	*H*-statistic	*p*-value	Significant?
Silicate:Nitrate	2	21	14.3	$p < 0.05$ ($7.9 \, e^{-4}$)	Yes
Fe:Nitrate	2	21	10.5	$p < 0.05$ (0.005)	Yes
Diversity (H')	2	20	10.4	$p < 0.05$ (0.005)	Yes

Appendix Table 1. (**1A**) Tests for data distribution normality for select variables. Non-normal data distributions are indicated in red font. Skewness, Kurtosis, Kolmogorov–Smirnov statistic (*D*) and *p*-value are reported. (**1B**) One-way ANOVA results from select variables with normal distributions. Test details include the degrees of freedom (*df*) for the test between groups and the test within groups. *F*-statistic, *p*-value, and significance classification are reported. (**1C**) Kruskal-Wallis results from non-normal data distributions. Test details include the degrees of freedom (*df*) for the test between groups and the number of observations (*N*). *H*-statistic, *p*-value, and significance classification are reported.

Appendix Table 2. Post hoc tests – Tukey's HSD and Dunn's			
Variables	**Eddy I vs. Eddy II**	**Eddy I vs. Non-eddy**	**Eddy II vs. Non-eddy**
Temperature	Q(3,18)=12.6; $p<0.01$ Significant	Q(3,18)=9.7; $p<0.01$ Significant	Q(3,18)=1.3; $p=0.6$ Not significant
Salinity	Q(3,18)=4.4; $p<0.05$ Significant	Q(3,18)=12.6; $p<0.01$ Significant	Q(3,18)=8.7; $p<0.01$ Significant
Fluorescence	Q(3,18)=0.3; $p=0.8$ Not significant	Q(3,18)=5.0; $p<0.01$ Significant	Q(3,18)=5.2; $p<0.01$ Significant
Nitrate	Q(3,18)=10.5; $p<0.01$ Significant	Q(3,18)=10.5; $p<0.01$ Significant	Q(3,18)=1.3; $p=0.6$ Not significant
Silicate	Q(3,18)=7.1; $p<0.01$ Significant	Q(3,18)=6.9; $p<0.01$ Significant	Q(3,18)=0.7; $p=0.9$ Not significant
Phosphate	Q(3,18)=12.0; $p<0.01$ Significant	Q(3,18)=11.3; $p<0.01$ Significant	Q(3,18)=0.8; $p=0.8$ Not significant
Rhizosolenia Relative Abundance	Q(3,17)=10.3; $p<0.01$ Significant	Q(3,17)=0.8; $p=0.8$ Not Significant	Q(3,17)=8.4; $p<0.01$ Significant
Wind Speed	Q(3,18)=12.4; $p<0.01$ Significant	Q(3,18)=7.8; $p<0.01$ Significant	Q(3,18)=3.0; $p=0.1$ Not significant
Density	Q(3,18)=14.7; $p<0.01$ Significant	Q(3,18)=16.5; $p<0.01$ Significant	Q(3,18)=3.7; $p<0.05$ Significant
Richness	$p=0.2$; Not significant	$p=0.2$; Not significant	$p=0.9$; Not significant
Silicate:Nitrate *	$p<0.01(0.008)$; Significant	$p<0.01(0.001)$; Significant	$p=0.3$; Not significant
dFe:Nitrate *	$p<0.05(0.002)$; Significant	$p<0.05(0.002)$; Significant	$p=0.7$; Not significant
Diversity (H') *	$p=0.1$; Not significant	$p=0.2$; Not significant	$p<0.01(0.005)$; Significant

**Appendix Table 2.** Results from the post hoc tests performed on the select variables. The normal distribution data were tested by the Tukey's honestly significant difference (HSD) post hoc test. Reported are the Q-statistic, p-value, and significance classification. (*) The non-normal distribution data were tested by the Dunn's post hoc test. Reported are p-values and significance classification.

| Species Classification	OTU name from NCBI	Accession Number	Match percentage	Total Reads
Rhizosolenia sp. 1	Rhizosolenia shubsholei 18S ribosomal RNA gene partial sequence	AY485510	91.0%	104,345
Fragilariopsis cf. kerguelensis	Fragilariopsis kerguelensis strain L26-C5 18S ribosomal RNA gene partial sequence	KJ866919	98.7%	44,196
Actinocyclus sp. MPA-2013	Actinocyclus sp. 1 MPA-2013 isolate ECT3899tinydrum 18S ribosomal RNA gene partial sequence	KC309522	**99.8%**	33,484
Asteromphalus sp. TN-2014	Asteromphalus sp. TN-2014 isolate ECT3832Aster 18S small subunit ribosomal RNA gene partial sequence	KJ577845	**99.7%**	30,210
Pseudo-nitzschia cf. sp. A3ni	Pseudo-nitzschia sp. A3ni 18S ribosomal RNA gene partial sequence	KJ671704	98.5%	23,831
Thalassiosira oestrupii var. venrickae	Thalassiosira oestrupii var. venrickae strain CC03-15 18S small subunit ribosomal RNA gene partial sequence	DQ514870	**99.7%**	20,904
Fragilariopsis kerguelensis	Fragilariopsis kerguelensis strain L26-C5 18S ribosomal RNA gene partial sequence	KJ866919	**99.1%**	14,130
Pseudo-nitzschia americana	Pseudo-nitzschia americana strain UNC1412 18S ribosomal RNA gene partial sequence	KX229689	**100%**	12,777
Pseudo-nitzschia sp. A3ni	Pseudo-nitzschia sp. A3ni 18S ribosomal RNA gene partial sequence	KJ671704	**99.3%**	11,659
Pseudo-nitzschia subcurvata	Pseudo-nitzschia subcurvata strain UNC1409 18S ribosomal RNA gene partial sequence	KX253952	**99.8%**	11,458
Brockmanniella brockmannii	Brockmanniella brockmannii gene for 18S ribosomal RNA partial sequence strain: NIES-3972	LC189090	**100%**	8,928
Cylindrotheca cf. closterium	Cylindrotheca closterium strain 10 18S ribosomal RNA gene partial sequence	KJ671694	97.4%	8,728
Thalassiothrix sp. 1	Thalassiothrix longissima gene for 18S rRNA partial sequence strain: p441	AB430611	96.7%	7,888
Rhizosolenia sp. 2	Rhizosolenia shubsholei 18S ribosomal RNA gene partial sequence	AY485510	92.7%	7,437
Chaetoceros sp. NIOZ	Chaetoceros sp. NIOZ 18S ribosomal RNA gene partial sequence	EF192996	**99.7%**	6,783
Thalassiosira oceanica	Thalassiosira oceanica 18S ribosomal RNA gene partial sequence	HM991696	**100%**	6,292
Pseudo-nitzschia delicatissima	Pseudo-nitzschia delicatissima strain SZN-B653 18S ribosomal RNA gene partial sequence	KJ608075	**100%**	5,832
Cylindrotheca sp. UTKSA0079	Cylindrotheca sp. isolate UTKSA0079 18S ribosomal RNA gene partial sequence	KX981848	**99.4%**	5,686
Rhizosolenia sp. 3	Rhizosolenia shubsholei 18S ribosomal RNA gene partial sequence	AY485510	94.1%	5,258
Thalassiosira ritscheri	Thalassiosira ritscheri strain LC01-12 18S small subunit ribosomal RNA gene partial sequence	DQ514891	**99.0%**	4,241

Appendix Table 3. Detailed OTU information, including species classifications used in this study, the name of the species from NCBI, accession number, match percentage, and total reads detected in all samples. Match percentages above 99% have been bolded.

48

Station Numbers

Species Name	1	2	3	4	5	6	7	8	9	10	11	12	14	15	16	17	18	19	21	22
Rhizosolenia sp. 1	1.1%	**64.1%**	**70.1%**	**42.5%**	**57.2%**	**71.0%**	**71.2%**	**44.4%**	**12.1%**	5.9%	0.2%	0.1%	6.6%	0.5%	1.3%	3.9%	0.0%	0.1%	0.0%	**20.0%**
Fragilariopsis cf. kerguelensis	**11.4%**	3.5%	2.6%	0.7%	0.8%	0.4%	0.7%	7.1%	7.3%	**14.5%**	**11.5%**	8.7%	5.0%	8.6%	**18.6%**	**22.0%**	**19.4%**	**29.2%**	**17.2%**	**19.1%**
Actinocyclus sp. 1	6.2%	7.4%	6.7%	6.1%	7.8%	4.3%	7.7%	9.7%	**16.8%**	5.7%	5.5%	**13.3%**	4.1%	3.6%	5.1%	**11.2%**	**13.0%**	9.8%	3.6%	6.7%
Asteromphalus sp. 1	4.4%	1.5%	1.2%	0.1%	0.4%	0.2%	0.3%	3.1%	9.1%	**10.6%**	8.2%	2.6%	**18.1%**	**22.5%**	**16.7%**	6.0%	5.0%	5.2%	**24.8%**	0.9%
Pseudo-nitzschia cf. sp.	4.2%	2.6%	3.3%	**29.4%**	**16.0%**	9.6%	5.9%	4.3%	3.8%	0.0%	0.4%	0.0%	2.4%	9.2%	7.1%	2.7%	1.8%	1.6%	2.6%	4.1%
Thalassiosira oestrupii var. venrickae	2.1%	3.6%	3.3%	0.5%	0.8%	0.4%	1.3%	3.4%	9.3%	2.7%	2.1%	1.4%	5.3%	**10.4%**	**13.2%**	7.5%	7.8%	7.3%	9.6%	6.4%
Fragilariopsis kerguelensis	2.2%	0.5%	0.4%	0.2%	0.1%	0.2%	0.1%	2.4%	1.4%	6.5%	3.5%	5.5%	1.6%	2.4%	6.2%	9.7%	6.1%	9.4%	3.7%	4.3%
Pseudo-nitzschia americana	2.3%	0.9%	1.2%	0.3%	0.2%	0.1%	0.5%	1.9%	5.5%	1.5%	1.6%	0.7%	1.5%	1.0%	1.9%	6.4%	8.9%	8.4%	8.0%	7.6%
Pseudo-nitzschia sp.	4.8%	0.9%	0.7%	0.2%	0.2%	0.8%	2.1%	1.1%	2.0%	0.0%	0.1%	0.3%	1.7%	**19.3%**	3.7%	4.2%	0.9%	3.7%	6.0%	3.6%
Pseudo-nitzschia subcurvata	**19.5%**	4.5%	2.0%	4.4%	0.8%	1.2%	1.1%	2.6%	1.4%	2.3%	1.1%	0.6%	0.7%	1.2%	2.8%	2.2%	0.9%	1.0%	0.6%	1.4%
Brockmanniella brockmannii	0.1%	0.3%	0.3%	0.1%	0.5%	0.2%	0.4%	0.9%	5.4%	8.6%	5.7%	1.3%	0.8%	0.3%	0.3%	2.4%	7.6%	3.6%	1.6%	1.3%
Cylindrotheca cf. closterium	0.7%	0.2%	0.1%	0.0%	0.1%	0.0%	0.0%	0.5%	1.6%	8.8%	**10.1%**	**14.7%**	0.6%	0.1%	0.0%	0.7%	0.4%	0.5%	0.6%	0.3%
Thalassiothrix sp. 1	0.4%	1.5%	1.1%	5.9%	6.0%	6.1%	3.1%	0.8%	1.9%	0.9%	1.2%	0.0%	2.3%	1.7%	1.8%	0.3%	0.3%	0.0%	0.6%	0.2%
Rhizosolenia sp. 2	1.4%	1.8%	1.4%	1.0%	3.5%	2.1%	2.1%	3.5%	2.6%	0.4%	2.2%	4.1%	2.8%	1.0%	0.9%	1.0%	0.2%	0.0%	0.3%	1.7%
Chaetoceros sp.	1.0%	0.2%	0.2%	0.1%	0.2%	0.1%	0.2%	1.3%	0.9%	**10.4%**	4.2%	3.4%	1.1%	0.9%	3.0%	0.7%	1.0%	0.7%	1.0%	0.7%
Thalassiosira oceanica	0.2%	0.1%	0.1%	0.0%	0.0%	0.0%	0.0%	0.4%	2.0%	3.5%	7.1%	0.0%	1.1%	0.6%	1.3%	2.6%	3.2%	2.8%	2.2%	2.1%
Pseudo-nitzschia delicatissima	3.0%	0.8%	0.3%	1.0%	0.33%	0.5%	0.2%	1.0%	2.8%	2.2%	2.3%	0.7%	1.6%	1.0%	1.2%	0.8%	0.5%	0.6%	2.1%	4.2%
Cylindrotheca sp.	**15.1%**	1.4%	0.4%	2.2%	0.1%	0.1%	0.3%	0.5%	0.8%	0.2%	0.7%	0.3%	0.6%	1.0%	0.3%	0.3%	0.2%	0.1%	0.9%	0.5%
Rhizosolenia sp. 3	0.7%	0.0%	0.0%	0.0%	0.0%	0.0%	0.0%	0.1%	1.0%	1.3%	4.8%	**11.9%**	3.1%	0.1%	0.1%	0.1%	0.0%	0.0%	0.3%	0.0%
Thalassiosira ritscheri	0.7%	0.5%	0.2%	0.6%	0.2%	0.1%	0.4%	0.3%	1.2%	0.0%	0.1%	0.0%	0.4%	2.3%	1.1%	2.1%	1.7%	2.1%	2.3%	4.1%
Other identified diatoms	**18.2%**	3.8%	4.3%	4.6%	4.6%	2.6%	2.3%	**10.7%**	**11.3%**	**13.9%**	**27.4%**	**30.5%**	**38.8%**	**12.3%**	**13.3%**	**13.1%**	**21.1%**	**14.0%**	**12.2%**	**10.7%**

Appendix Table 4. Relative abundances for the top 20 OTUs at each station. Percentages above 10% have been bolded.
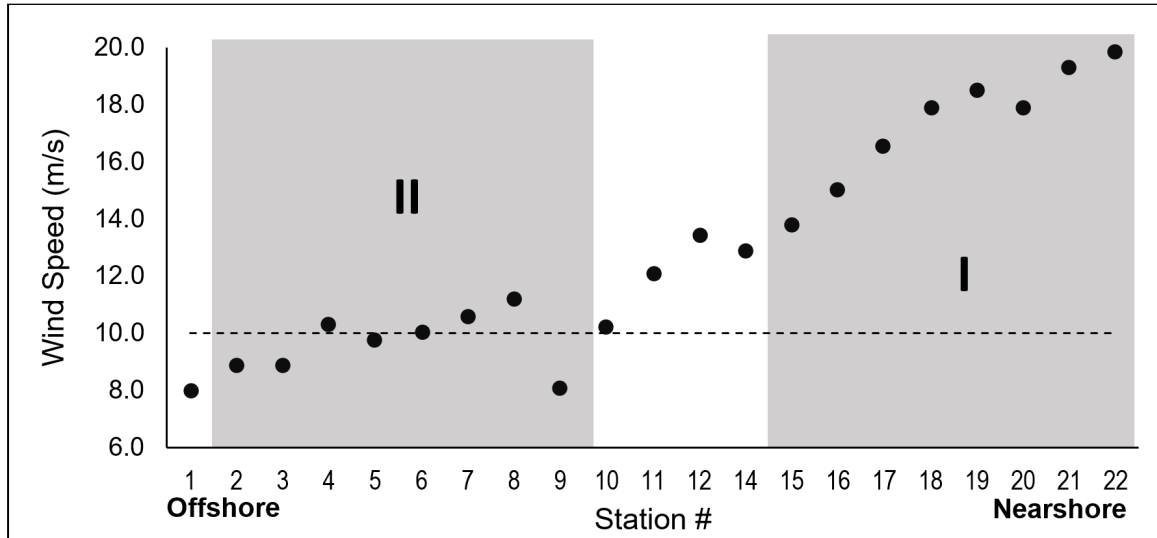
Appendix Figure 1. Wind speed measurements at each station. The dashed line (10 m/s) indicates the estimated maximum wind speed tolerated by *Rhizosolenia* mats.
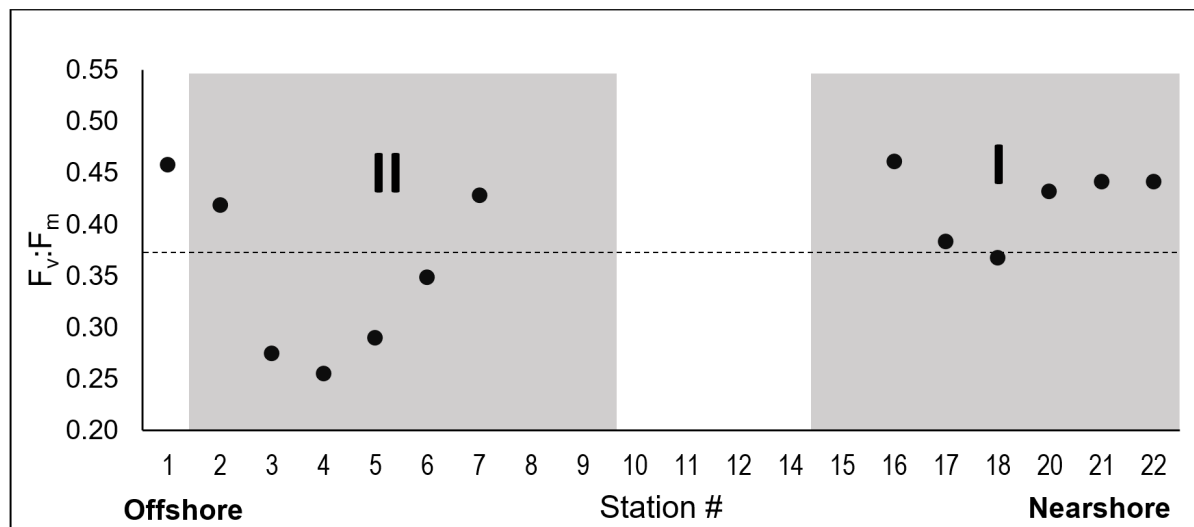
Appendix Figure 2. Variable fluorescence (F_v)/Maximum fluorescence (F_m) used to estimate photosynthetic efficiency of primary producers in surface waters. Values above the dashed line are those indicating high photosynthetic efficiency. Measurements taken during daytime have been removed. Grey boxes demarcate the boundaries of eddies I and II.
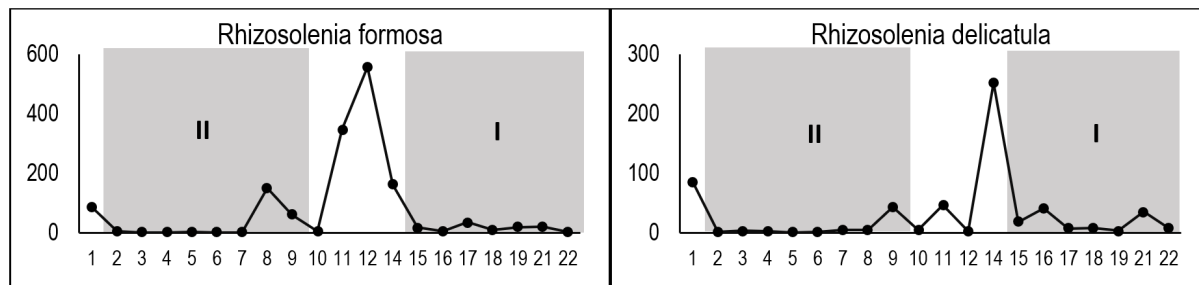
Appendix Figure 3. Line graphs of the Rhizosolenia species not categorized among the top 20 OTUs. Total reads are shown across the stations.
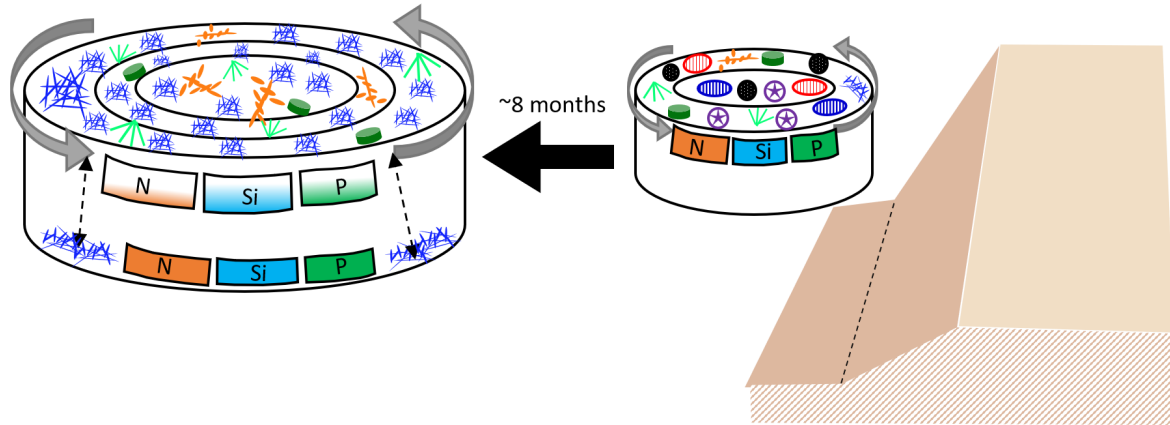
Appendix Figure 4. Representation of the ecological succession that occurs during eddy aging and propagation offshore. Eddy I is the cylindrical feature spinning counterclockwise on the right side; the eastern boundary of this eddy is located above the continental shelf, shown here as the beige boxes. On the surface of eddy I, there is a diverse community of diatoms, shown in the colors corresponding to those in the community composition columns (Figure 7). The three boxes on the front of eddy I represent the high-nutrient coastal environment with replete levels of nitrate, silicate, and phosphate. Eddy II is the cylindrical shape on the left side, also spinning counterclockwise, and represents a time-lapse of 8 months after eddy I. On the surface of eddy II, there is a low-diversity community of diatoms dominated by *Rhizosolenia* (blue mats) in a low-nutrient environment. Mats access nutrient-replete waters below the euphotic zone by vertically migrating, as shown by the arrows.

REFERENCES

Aizawa, C., Tanimoto, M., & Jordan, R. W. (2005). Living diatom assemblages from North
Pacific and Bering Sea surface waters during summer 1999. *Deep Sea Research Part II:
Topical Studies in Oceanography, 52*, 2186-2205. doi:10.1016/j.dsr2.2005.08.008

Alldredge, A., & Silver, M. (1982). Abundance and production rates of floating diatom mats
(*Rhizosolenia castracanei* and *R. imbricata var. shrubsolei*) in the Eastern Pacific Ocean.
Marine Biology, 66, 83-88.

Altschul, S. F., Gish, W., Miller, W., Myers, E. W., & Lipman, D. J. (1990). Basic local
alignment search tool. *Journal of molecular biology, 215*, 403-410.

Anderson, E. E., Wilson, C., Knap, A. H., & Villareal, T. A. (2018). Summer diatom blooms in
the eastern North Pacific gyre investigated with a long-endurance autonomous surface
vehicle. *PeerJ, 6*, e5387.

Batteen, M. L., Cipriano, N. J., & Monroe, J. T. (2003). A large-scale seasonal modeling study of
the California Current System. *Journal of Oceanography, 59*, 545-562.

Benitez-Nelson, C. R., Bidigare, R. R., Dickey, T. D., Landry, M. R., Leonard, C. L., Brown, S.
L., . . . Becker, J. W. (2007). Mesoscale eddies drive increased silica export in the
subtropical Pacific Ocean. *Science, 316*, 1017-1021.

Bibby, T. S., Gorbunov, M. Y., Wyman, K. W., & Falkowski, P. G. (2008). Photosynthetic
community responses to upwelling in mesoscale eddies in the subtropical North Atlantic
and Pacific Oceans. *Deep Sea Research Part II: Topical Studies in Oceanography, 55*,
1310-1320.

Bilger, W., Schreiber, U., & Bock, M. (1995). Determination of the quantum efficiency of photosystem II and of non-photochemical quenching of chlorophyll fluorescence in the field. *Oecologia, 102*, 425-432.

Biller, D. V., & Bruland, K. W. (2014). The central California Current transition zone: A broad region exhibiting evidence for iron limitation. *Progress in Oceanography, 120*, 370-382. doi:10.1016/j.pocean.2013.11.002

Bowler, C., Vardi, A., & Allen, A. E. (2010). Oceanographic and biogeochemical insights from diatom genomes. *Annual Review Marine Science, 2*, 333-365. doi:10.1146/annurev-marine-120308-081051

Bray, J. R., & Curtis, J. T. (1957). An ordination of the upland forest communities of southern Wisconsin. *Ecological monographs, 27*, 325-349.

Brown, S. L., Landry, M. R., Selph, K. E., Yang, E. J., Rii, Y. M., & Bidigare, R. (2008). Diatoms in the desert: Plankton community response to a mesoscale eddy in the subtropical North Pacific. *Deep Sea Research Part II: Topical Studies in Oceanography, 55*, 1321-1333.

Bruland, Rue, E. L., & Smith, G. J. (2001). Iron and macronutrients in California coastal upwelling regimes: Implications for diatom blooms. *Limnology and Oceanography, 46*, 1661-1674.

Bruland, Rue, E. L., Smith, G. J., & DiTullio, G. R. (2005). Iron, macronutrients and diatom blooms in the Peru upwelling regime: brown and blue waters of Peru. *Marine Chemistry, 93*, 81-103. doi:10.1016/j.marchem.2004.06.011

Brzezinski, M. A. (1985). The Si: C: N ratio of marine diatoms: interspecific variability and the effect of some environmental variables. *Journal of Phycology, 21*, 347-357.

Capone, D. G., & Hutchins, D. A. (2013). Microbial biogeochemistry of coastal upwelling

    regimes in a changing ocean. *Nature Geoscience, 6*, 711-717. doi:10.1038/ngeo1916

Carpenter, E. J. (1977). *Rhizosolenia* mats. *Limnology and Oceanography, 22*, 739-741.

Chappell, P. D., Armbrust, E. V., Barbeau, K. A., Bundy, R. M., Moffett, J. W., Vedamati, J., &

    Jenkins, B. D. (2019). Patterns of diatom diversity correlate with dissolved trace metal

    concentrations and longitudinal position in the northeast Pacific coastal-offshore

    transition zone. *Marine Ecology Progress Series, 609*, 69-86.

Chavez, F. P., Barber, R. T., Kosro, P. M., Huyer, A., Ramp, S. R., Stanton, T. P., & Rojas de

    Mendiola, B. (1991). Horizontal transport and the distribution of nutrients in the coastal

    transition zone off northern California: effects on primary production, phytoplankton

    biomass and species composition. *Journal of Geophysical Research: Oceans, 96*, 14833-

    14848.

Chenillat, F., Franks, P. J., Capet, X., Rivière, P., Grima, N., Blanke, B., & Combes, V. (2018).

    Eddy properties in the Southern California Current System. *Ocean Dynamics, 68*, 761-

    777.

Chenillat, F., Franks, P. J., & Combes, V. (2016). Biogeochemical properties of eddies in the

    California Current System. *Geophysical Research Letters, 43*, 5812-5820.

Chenillat, F., Franks, P. J., Rivière, P., Capet, X., Grima, N., & Blanke, B. (2015). Plankton

    dynamics in a cyclonic eddy in the Southern California Current System. *Journal of

    Geophysical Research: Oceans, 120*, 5566-5588.

Combes, V., Chenillat, F., Di Lorenzo, E., Rivière, P., Ohman, M., & Bograd, S. (2013). Cross-

    shore transport variability in the California Current: Ekman upwelling vs. eddy dynamics.

    Progress in Oceanography, 109, 78-89.

Crawford, R. M., Hinz, F., & Koschinski, P. (2000). The combination of *Chaetoceros gaussii* (Bacillariophyta) with *Attheya*. *Phycologia, 39*, 238-244.

Du, X., & Peterson, W. T. (2013). Seasonal cycle of phytoplankton community composition in the coastal upwelling system off central Oregon in 2009. *Estuaries and Coasts, 37*, 299-311. doi:10.1007/s12237-013-9679-z

Ducklow, H. W., Steinberg, D. K., & Buesseler, K. O. (2001). Upper ocean carbon export and the biological pump. *Oceanography. 14*, 50-58.

Dunn, O. J. (1964). Multiple comparisons using rank sums. *Technometrics, 6*, 241-252.

Engel, A., Goldthwait, S., Passow, U., & Alldredge, A. (2002). Temporal decoupling of carbon and nitrogen dynamics in a mesocosm diatom bloom. *Limnology and Oceanography, 47*, 753-761.

Eren, A. M., Morrison, H. G., Lescault, P. J., Reveillaud, J., Vineis, J. H., & Sogin, M. L. (2015). Minimum entropy decomposition: Unsupervised oligotyping for sensitive partitioning of high-throughput marker gene sequences. *International Society for Microbial Ecology, 9*, 968-979. doi:10.1038/ismej.2014.195

Falkowski, P. G. (1994). The role of phytoplankton photosynthesis in global biogeochemical cycles. *Photosynthesis Research, 39*, 235-258. doi:10.1007/BF00014586

Falkowski, P. G. (1995). Ironing out what controls primary production in the nutrient-rich waters of the open-ocean. *Global Change Biology, 1*, 161-163. doi:DOI 10.1111/j.1365-2486.1995.tb00017.x

Falkowski, P. G., Barber, R. T., & Smetacek, V. V. (1998). Biogeochemical controls and feedbacks on ocean primary production. *Science, 281*, 200-207. doi:10.1126/science.281.5374.200

Fisher, R. A. (1921). On the 'probable error' of a coefficient of correlation deduced from a small sample. *Metron, 1*, 1-32.

Foster, R. A., Kuypers, M. M., Vagner, T., Paerl, R. W., Musat, N., & Zehr, J. P. (2011). Nitrogen fixation and transfer in open ocean diatom-cyanobacterial symbioses. *International Society for Microbial Ecology, 5*, 1484-1493. doi:10.1038/ismej.2011.26

Goebel, N., Edwards, C., Zehr, J., Follows, M., & Morgan, S. (2013). Modeled phytoplankton diversity and productivity in the California Current System. *Ecological modelling, 264*, 37-47.

Hardge, K., Peeken, I., Neuhaus, S., Lange, B. A., Stock, A., Stoeck, T., . . . Metfies, K. (2017). The importance of sea ice for exchange of habitat-specific protist communities in the Central Arctic Ocean. *Journal of Marine Systems, 165*, 124-138.

Heil, C. A., Revilla, M., Glibert, P. M., & Murasko, S. (2007). Nutrient quality drives differential phytoplankton community composition on the southwest Florida shelf. *Limnology and Oceanography, 52*, 1067-1078.

Hood, R. R., Abbott, M. R., Huyer, A., & Kosro, P. M. (1990). Surface patterns in temperature, flow, phytoplankton biomass, and species composition in the coastal transition zone off northern California. *Journal of Geophysical Research: Oceans, 95*, 18081-18094.

Hoover, S. M., & Tréhu, A. M. (2017). Uplift, emergence, and subsidence of the Gorda escarpment basement ridge offshore Cape Mendocino, CA. *Geochemistry, Geophysics, Geosystems, 18*, 4503-4521.

Kaczmarska, I., Lovejoy, C., Potvin, M., & Macgillivary, M. (2009). Morphological and molecular characteristics of selected species of *Minidiscus* (Bacillariophyta, Thalassiosiraceae). *European Journal of Phycology, 44*, 461-475.

Kemp, A. E., & Villareal, T. A. (2013). High diatom production and export in stratified waters–

 A potential negative feedback to global warming. *Progress in Oceanography, 119*, 4-23.

Kooistra, W. H., Gersonde, R., Medlin, L. K., & Mann, D. G. (2007). The origin and evolution

 of the diatoms: their adaptation to a planktonic existence. *Evolution of Primary*

 Producers in the Sea, 207-249.

Kooistra, W. H., Sarno, D., Balzano, S., Gu, H., Andersen, R. A., & Zingone, A. (2008). Global

 diversity and biogeography of *Skeletonema* species (Bacillariophyta). *Protist, 159*, 177-

 193. doi:10.1016/j.protis.2007.09.004

Kruskal, W. H., & Wallis, W. A. (1952). Use of ranks in one-criterion variance analysis. *Journal*

 of the American Statistical Association, 47, 583-621.

Kurian, J., Colas, F., Capet, X., McWilliams, J. C., & Chelton, D. B. (2011). Eddy properties in

 the California Current System. *Journal of Geophysical Research: Oceans, 116*, C08027.

Lachkar, Z., & Gruber, N. (2012). A comparative study of biological production in eastern

 boundary upwelling systems using an artificial neural network. *Biogeosciences, 9*, 293-

 308.

Lassiter, A. M., Wilkerson, F. P., Dugdale, R. C., & Hogue, V. E. (2006). Phytoplankton

 assemblages in the CoOP-WEST coastal upwelling area. *Deep Sea Research Part II:*

 Topical Studies in Oceanography, 53, 3063-3077.

Letscher, R. T., & Villareal, T. A. (2018). Evaluation of the seasonal formation of subsurface

 negative preformed nitrate anomalies in the subtropical North Pacific and North Atlantic.

 Biogeosciences, 15, 6461-6480.

Lewitus, E., Bittner, L., Malviya, S., Bowler, C., & Morlon, H. (2018). Clade-specific

diversification dynamics of marine diatoms since the Jurassic. *Nature Ecology &*

Evolution, 2, 1715.

Lilliefors, H. W. (1967). On the Kolmogorov-Smirnov test for normality with mean and variance

unknown. *Journal of the American Statistical Association, 62*, 399-402.

Mann, D. G., & Droop, S. (1996). Biodiversity, biogeography and conservation of diatoms.

*Biogeography of Freshwater Algae,*19-32.

Mann, D. G., & Vanormelingen, P. (2013). An inordinate fondness? The number, distributions,

and origins of diatom species. *Journal of Eukaryotic Microbiology, 60*, 414-420.

Marchesiello, P., McWilliams, J. C., & Shchepetkin, A. (2003). Equilibrium structure and

dynamics of the California Current System. *Journal of Physical Oceanography, 33*, 753-

783.

Marchetti, A., Maldonado, M. T., Lane, E. S., & Harrison, P. J. (2006). Iron requirements of the

pennate diatom *Pseudo-nitzschia*: Comparison of oceanic (high-nitrate, low-chlorophyll

waters) and coastal species. *Limnology and Oceanography, 51*, 2092-2101.

Martin, C. L., & Tortell, P. D. (2008). Bicarbonate transport and extracellular carbonic

anhydrase in marine diatoms. *Physiologia Plantarum, 133*, 106-116.

Martínez, L., Silver, M. W., King, J. M., & Alldredge, A. L. (1983). Nitrogen fixation by

floating diatom mats: A source of new nitrogen to oligotrophic ocean waters. *Science,*

221, 152-154.

Massey, F. J. (1951). The Kolmogorov-Smirnov test for goodness of fit. *Journal of the American*

Statistical Association, 46, 68-78.

Mellett, T., Brown, M. T., Chappell, P. D., Duckham, C., Fitzsimmons, J. N., Till, C. P., . . .

    Buck, K. N. (2018). The biogeochemical cycling of iron, copper, nickel, cadmium,

    manganese, cobalt, lead, and scandium in a California Current experimental study.

    Limnology and Oceanography, 63, S425-S447. doi:10.1002/lno.10751

Murchie, E. H., & Lawson, T. (2013). Chlorophyll fluorescence analysis: A guide to good

    practice and understanding some new applications. *Journal of Experimental Botany, 64*,

    3983-3998.

Nagai, T., Gruber, N., Frenzel, H., Lachkar, Z., McWilliams, J. C., & Plattner, G. K. (2015).

    Dominant role of eddies and filaments in the offshore transport of carbon and nutrients in

    the California Current System. *Journal of Geophysical Research: Oceans, 120*, 5318-

    5341.

Owen, R. (1980). Eddies of the California Current System: Physical and ecological

    Characteristics. *The California Islands: Proceedings of a Multidisciplinary Symposium*,

    237–263.

Parsons, T. R., Maita, Y., & Lalli, C. M. (1984). A manual of chemical and biological methods

    for seawater analysis. *Oxford: Pergamon*, *1*, 173.

Pearson, K. (1905). Das fehlergesetz und seine verallgemeiner-ungen durch Fechner und

    Pearson. *Biometrika, 4*, 169-212.

Peterson, W. T., Fisher, J. L., Strub, P. T., Du, X., Risien, C., Peterson, J., & Shaw, C. T. (2017).

    The pelagic ecosystem in the Northern California Current off Oregon during the 2014–

    2016 warm anomalies within the context of the past 20 years. *Journal of Geophysical*

    Research: Oceans, 122, 7267-7290.

Pilskaln, C. H., Villareal, T. A., Dennett, M., Darkangelo-Wood, C., & Meadows, G. (2005). High concentrations of marine snow and diatom algal mats in the North Pacific Subtropical Gyre: Implications for carbon and nitrogen cycles in the oligotrophic ocean. *Deep Sea Research Part I: Oceanographic Research Papers, 52*, 2315-2332.

Richardson, T. L., Ciotti, A. M., Cullen, J. J., & Villareal, T. A. (1996). Physiological and optical properties of *Rhizosolenia formosa* (Bacillariophyceae) in the context of open-ocean vertical migration. *Journal of Phycology, 32*, 741-757.

Richardson, T. L., Cullen, J. J., Kelley, D. E., & Lewis, M. R. (1998). Potential contributions of vertically migrating *Rhizosolenia* to nutrient cycling and new production in the open ocean. *Journal of Plankton Research, 20*, 219-241.

Sancetta, C. (1995). Diatoms in the Gulf of California: Seasonal flux patterns and the sediment record for the last 15,000 years. *Paleoceanography, 10*, 67-84.

Schloss, P. D., Westcott, S. L., Ryabin, T., Hall, J. R., Hartmann, M., Hollister, E. B., . . . Weber, C. F. (2009a). Introducing mothur: open-source, platform-independent, community-supported software for describing and comparing microbial communities. *Applied Environmental Microbiology, 75*, 7537-7541. doi:10.1128/AEM.01541-09

Schloss, P. D., Westcott, S. L., Ryabin, T., Hall, J. R., Hartmann, M., Hollister, E. B., . . . Weber, C. F. (2009b). Introducing mothur: Open-Source, Platform-Independent, Community-Supported Software for Describing and Comparing Microbial Communities. *Applied and Environmental Microbiology, 75*, 7537-7541.

Shannon, C. E. (1948). A mathematical theory of communication. *Bell System Technical Journal, 27*, 623-656.

Singler, H. R., & Villareal, T. A. (2005). Nitrogen inputs into the euphotic zone by vertically migrating *Rhizosolenia* mats. *Journal of Plankton Research, 27*, 545-556.

Smith, G. A. (1999). Creating a public of environmentalists. *Ecological education in action: On weaving education, culture, and the environment*, 207.

Sumper, M., & Brunner, E. (2006). Learning from diatoms: Nature's tools for the production of nanostructured silica. *Advanced Functional Materials, 16*, 17-26. doi:10.1002/adfm.200500616

Till, C., Solomon, J., Cohen, N., Lampe, R., Marchetti, A., Coale, T., & Bruland, K. (2019). The iron limitation mosaic in the California Current System: Factors governing Fe availability in the shelf/near-shelf region. *Limnology and Oceanography, 64*, 109-123.

Tomas, C. R. (Ed.). (1997). *Identifying Marine Phytoplankton*. San Diego: Academic Press.

Tukey, J. W. (1976). *Exploratory data analysis*. Massachusetts: Addison-Wesley.

Vanormelingen, P., Verleyen, E., & Vyverman, W. (2007). The diversity and distribution of diatoms: from cosmopolitanism to narrow endemism. In *Protist Diversity and Geographical Distribution*, 159-171.

Venrick, E. (1971). Recurrent groups of diatom species in the North Pacific. *Ecology, 52*, 614-625.

Venrick, E. (2009). Floral patterns in the California Current: The coastal-offshore boundary zone. *Journal of Marine Research, 67*, 89-111.

Villareal, T. A. (1987). Evaluation of nitrogen fixation in the diatom genus *Rhizosolenia* Ehr. in the absence of its cyanobacterial symbiont *Richelia intracellularis* Schmidt. *Journal of Plankton Research, 9*, 965-971.

Villareal, T. A., Adornato, L., Wilson, C., & Schoenbaechler, C. A. (2011). Summer blooms of

    diatom-diazotroph assemblages and surface chlorophyll in the North Pacific gyre: A

    disconnect. *Journal of Geophysical Research: Oceans, 116*.

Villareal, T. A., & Carpenter, E. J. (1989). Nitrogen fixation, suspension characteristics, and

    chemical composition of *Rhizosolenia* mats in the central North Pacific gyre. *Biological*

    Oceanography, 6, 327-345.

Villareal, T. A., Pilskaln, C. H., Montoya, J. P., & Dennett, M. (2014). Upward nitrate transport

    by phytoplankton in oceanic waters: Balancing nutrient budgets in oligotrophic seas.

    PeerJ, 2, e302.

Villareal, T. A., Woods, S., Moore, J. K., & CulverRymsza, K. (1996). Vertical migration of

    Rhizosolenia mats and their significance to NO3-fluxes in the central North Pacific gyre.

    Journal of Plankton Research, 18, 1103-1121.

Visco, J. A., Apotheloz-Perret-Gentil, L., Cordonier, A., Esling, P., Pillet, L., & Pawlowski, J.

    (2015). Environmental monitoring: Inferring the diatom index from next-generation

    sequencing data. *Environmental Science and Technology, 49*, 7597-7605.

    doi:10.1021/es506158m

Westfall, P. H. (2014). Kurtosis as peakedness, 1905–2014. RIP. *The American Statistician, 68*,

    191-195.

Wilson, C., & Qiu, X. (2008). Global distribution of summer chlorophyll blooms in the

    oligotrophic gyres. *Progress in Oceanography, 78*, 107-134.

    doi:10.1016/j.pocean.2008.05.002

Wilson, C., Villareal, T. A., Maximenko, N., Bograd, S. J., Montoya, J. P., & Schoenbaechler, C. A. (2008). Biological and physical forcings of late summer chlorophyll blooms at 30 N in the oligotrophic Pacific. *Journal of Marine Systems, 69*, 164-176.

Zimmermann, J., Glockner, G., Jahn, R., Enke, N., & Gemeinholzer, B. (2015). Metabarcoding vs. morphological identification to assess diatom diversity in environmental studies. *Molecular Ecology Resources, 15*, 526-542. doi:10.1111/1755-0998.12336

Zimmermann, J., Jahn, R., & Gemeinholzer, B. (2011). Barcoding diatoms: evaluation of the V4 subregion on the 18S rRNA gene, including new primers and protocols. *Organisms Diversity & Evolution, 11*, 173-192. doi:10.1007/s13127-011-0050-6

VITA

Zuzanna Maria Abdala
Old Dominion University
Department of Ocean, Earth and Atmospheric Sciences
4600 Elkhorn Avenue, Norfolk, VA 23529 USA

EDUCATION

Master of Science: Ocean and Earth Sciences, Biological Oceanography Concentration, Old Dominion University, Norfolk, VA | May 2020

Thesis: *Diatom community composition shifts driven by coherent cyclonic mesoscale eddies in the California Current System.*

Bachelor of Arts: Biology, George Mason University, Fairfax, VA | May 2014

Senior Thesis: *A comparative foodweb and stable isotope analysis of the stomach contents of fish from Gunston Cove and Hunting Creek, VA.*

PUBLICATIONS

Abdala, ZM, S Clayton, SV Einarsson, K Powell, CP Till, TH Coale, PD Chappell. Diatom community composition shifts driven by coherent cyclonic mesoscale eddies in the California Current System. *In Prep*.

PROFESSIONAL EXPERIENCE

NSF Graduate Research Fellow: Old Dominion University, Department of Ocean, Earth, and Atmospheric Sciences, Norfolk, VA | June 2017 – May 2020

NSF Graduate Research Intern, Survey Analyst: NOAA, National Marine Fisheries Service, Office of Science and Technology, Economics and Social Analysis Division, Silver Spring, MD | June 2019 – January 2020

National Sea Grant Knauss Marine Policy Fellow, Habitat Science and Policy Analyst: NOAA, National Marine Fisheries Service, Office of Habitat Conservation, Restoration Center, Silver Spring, MD | February 2020 – February 2021